Luminescent indium phosphide nanocrystals formed from single-source precursors using fluoride-containing ionic liquids

by

Stephanie K. Lee

B.A., Austin College, 2014

A THESIS

submitted in partial fulfillment of the requirements for the degree

MASTER OF SCIENCE

Department of Chemistry
College of Arts and Sciences

KANSAS STATE UNIVERSITY
Manhattan, Kansas

2018

Approved by:

Major Professor
Emily McLaurin

Copyright

Abstract

Quantum dot (QD) or semiconductor nanocrystal research has propagated extensively over the past few years due to increasing interest in long lasting, renewable, and safe applications such as solar cells and LEDs. Quantum dots are utilized for their size dependent optical properties that are based on the quantum confinement effect. Cadmium-based materials dominated early quantum dot research, which led to honing of syntheses and expansion of our understanding of various mechanisms. Recently, however, current applications, such as solar cells, LEDs, and displays, for everyday consumers require less toxic materials. Indium phosphide (InP) is a possible substitute for cadmium-based materials as it is not intrinsically toxic and emits in the visible region from 450-700 nm.

Despite the potential benefits to using indium phosphide, reproducible synthetic methods for obtaining stable QDs with narrow size distribution and high quantum yield still need to be refined. Using single-source precursors such as magic-sized clusters is a good starting place for addressing some of these challenges. InP magic-sized clusters are stable intermediates that are homogenously sized and readily isolable for later growth into InP nanocrystals. Our goal with the InP clusters was to determine their long-term stability and reproducibility as an InP precursor. The InP clusters are can be reproduced, have longer stability when stored as a solid, and we can produce luminescent nanocrystals.

Producing highly luminescent InP nanocrystals without the use of HF or shell growth is a challenge. We used the 1-methyl-3-butylimidazolium tetrafluoroborate as our ionic liquid to determine the effect of various ratios of ionic liquid to an InP separate-source precursor on quantum yield. The 1:10 ratio of precursor to ionic liquid provided the highest quantum yield of 21%. These reactions were difficult to reproduce, because there were many factors that affected

the synthesis, such as how soon the precursor is used, when the reactions are conducted in the microwave, and how the ionic liquid interacts with the microwave. When using 1-methyl-3-butylimidazolium hexafluorophosphate as our ionic liquid and the magic-sized cluster precursor, there was a spike in pressure in the microwave, and the reaction could not proceed due to the production of a gas. This ionic liquid is still capable of producing nanocrystals with an absorption feature.

Understanding the mechanism of how these ionic liquids improve luminescence can lead to safer and more efficient syntheses. Ligand stripping and exchange is also a valuable tool for uncovering information about the surface chemistry. The Lewis acid, BF_3, formed adducts with native surface ligands and produces polar, stable nanocrystals. Refining the precursor synthesis so that it's reproducible and producing luminescent nanocrystals were both time consuming processes. This work serves an entry into understanding the process of surface passivation and surface composition of the luminescent InP nanocrystals produced with magic-sized clusters and ionic liquids.

Table of Contents

List of Figures

List of Tables

Acknowledgements

First, I would like to thank my research advisor, Emily McLaurin, for her support and guidance over the past 3 years. She clearly has a deep appreciation and understanding of our field, and I am grateful for the opportunity to work in her lab. I would also like to thank my labmates over the past few years for their help in the lab: Dr. Nate Coleman, Bemnet Kebede, Raghavender Siramdas, and Mohammad Yazdanparast. Our undergrads: Cesar Aparicio, Lacey Beck, Jacob Iverson, Will Jeffries, and Joenisse Rosado. I am especially glad that I became good friends with Lacey and Joenisse, as they made time in the lab a lot more enjoyable. I am also glad for my friends in chemistry and in other departments. I've made a lot of connections in various organizations (AXS, KAWSE, KSCI) throughout grad school. The people in these groups made my time in grad school more enriching and memorable.

I would like to thank my undergraduate research advisor, Stephanie Gould. I am grateful for her unwavering support through college and graduate school. I am glad she decided to give me the opportunity to work in her lab as a sophomore in college, even when I had not taken organic chemistry. I am especially grateful for my closest friends from various parts of my life: Ilish, Julie and Shelbi. I could not have gotten through grad school without them. I am fortunate to have a family that loves me unconditionally. I would especially like to thank the people that I've become close to during my final year here for their support. They have made leaving this place difficult, and I am grateful for the experiences and memories we've had here.

List of Abbreviations

QDs	Quantum dots
InPA	Indium palmitate
FT-IR	Fourier-transform infrared spectroscopy
UV-Vis	Ultraviolet-visible
PL	Photoluminescence
NC	Nanocrystal
InMA	Indium myristate
MAIL	Microwave-assisted ionic liquid
MSC	Magic-sized cluster
NC	Nanocrystal
$P(TMS)_3$	Tristrimethylsilylphosphine
MW	Microwave
QY	Quantum Yield

Chapter 1 - Introduction

1.1 Quantum Dots

Research on semiconductor nanocrystals or quantum dots has expanded to a variety of materials since they were first synthesized by Louis E. Brus in 1983.[1] Increased use of quantum dots from II-IV and III-V materials has led to commercial development. Their applications range from TVs[2] to solar cells[3,4] to biological imaging.[5–7] Recently, quantum dots were introduced to LED TVs by Samsung.[8] Many of these applications require narrow emission peaks and high quantum yields. Popular II-VI nanocrystals, such as CdSe, have achieved high quantum yields and narrow size distributions, however, these toxic-heavy-metal materials are not viable for long term use.[9] Indium phosphide (InP) is a good alternative to consider as it emits across the visible region and is not intrinsically toxic. Because the toxicity of quantum dots is not fully established, focusing on the synthetic challenges of indium phosphide is important in creating stable, less toxic, highly luminescent, and uniformly sized nanocrystals.[10]

1.2 Quantum Confinement Effect

Quantum dots grow in all directions and are known as zero dimensional structures.[11,12] As the diameters of these materials approach their Bohr radius, the density of electronic states decreases and when the size increases, the size of the band gap decreases. This is depicted in Figure 1. This band gap size-dependence is quantum confinement of the exciton and results in discrete energy transitions in the absorption and photoluminescence (PL). For example, as the nanocrystal size gets smaller, the absorption and PL blue shift to smaller wavelengths.

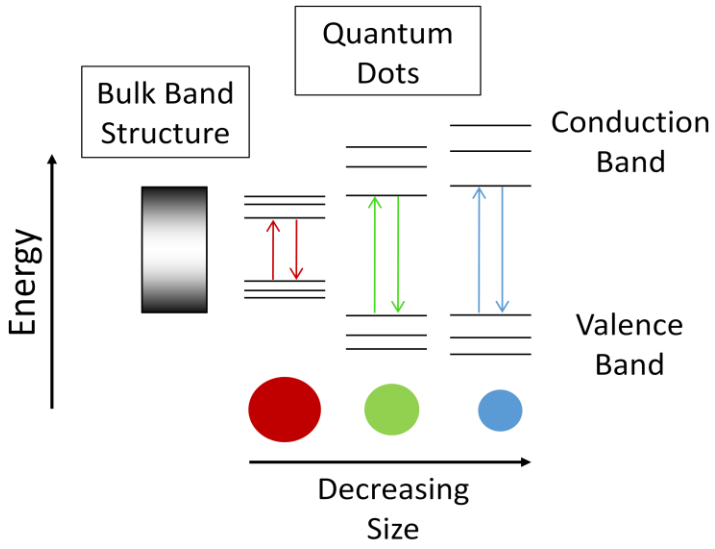

Figure 1. Cartoon visualization of the relationship between nanocrystal size and bandgap energy.

Indium-based quantum dots, specifically InP, are an appealing alternative to toxic-heavy-metal materials (lead and cadmium chalcogenides) because they are intrinsically less toxic.[13] Toxicity for nanocrystals in general depends on their size and composition.[9] Bulk InP has a 1.34 eV bandgap and exciton Bohr radius of 10 nm that allows for tunable emission in the visible region and is a direct bandgap material, so it can have more narrow absorption and emission.[12] In comparison to research done on the synthesis of cadmium-based materials, InP is behind in terms of quantum yield, size-distribution, and surface chemistry.[10] There are several aspects that can be addressed to improve luminescent properties, such as selection of precursor and modification of the surface.[10,14,15] Surface characteristics, such as ligand choice and surface traps, are highly important in determining the PL of the nanocrystal.[16] Using a stable, atomically precise precursor such as a magic-sized cluster can result in more controlled syntheses and surfaces.[16,17]

1.3 Magic-Sized Clusters as InP Precursors

Single-source precursors contain preformed bonds that can lead to more uniform nanocrystals reproducibly.[16,18] Magic-sized clusters (MSCs) are stable intermediates that exist prior to the formation of InP nanocrystals. InP MSCs are unique single-source precursors that have atomically precise structures. Xie *et al*. first reported the use of InP MSCs in a study of InP synthesis kinetics from molecular precursors.[19] Yang *et al*. used MSCs as an InP precursor for InP/ZnS QDs obtaining QYs as high as 60%.[20] They did not structurally characterize the yellow material. The Cossairt group determined the structure of the cluster, which is 1.3 nm in diameter.[21] The cluster core is shown in **Error! Reference source not found.**. Within the lattice, ndium or phosphorous are in a pseudo-tetrahedral holes. MSCs with carboxylate ligands grow into InP QDs through heterogenous growth, from one size to another and the carboxylate ligands can have multiple binding modes.[17,21] Their growth occurs via dissolution and then a second nucleation event. The established cluster provides more synthetic control for reproducing InP QDs as there are pre-formed bonds that deter the formation of unwanted side products. When synthesizing the clusters, the Cossairt group has also demonstrated that the InP cluster is stable across different temperatures and various precursor concentrations. It can also be customized with different carboxylate ligands or amines to improve quantum yield. In this work, we use the InP cluster along with ionic liquids to produce luminescent nanocrystals.

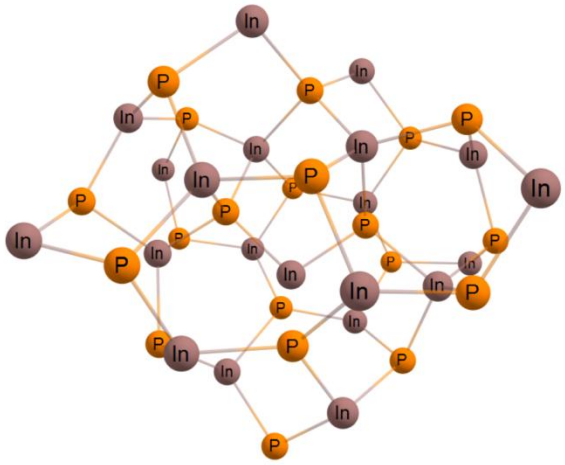

Figure 2. $In_{21}P_{20}$ cluster core crystal structure (adapted from reference 21) that was discovered by Cossairt and co-workers**.**

1.4 Microwave-Assisted Ionic Liquid Synthesis

Traditionally, quantum dots are produced using convective methods.[10,22] Due to the nature of the reactants, high temperatures are needed to proceed with nucleation.[9] During a standard hot-injection procedure, precursors are quickly injected to a heated, liquid reaction to spontaneously initiate the nucleation process by increasing the precursor concentration.[22] After nucleation, the solution is quickly quenched through cooling at room temperature and a decrease in monomer concentration. Because the hot-injection process is conducted in a flask heated by an oil bath or heating mantle, some control of the reaction conditions, such as rate and nucleation, is relinquished. This results in uneven thermal gradients that cause sample inhomogeneity and low quantum yields. Unwanted side products can also form with carboxylate and phosphorous precursors during a hot-injection reaction.

Lower quantum yields in InP nanocrystals can be attributed to phosphorous dangling bonds on the InP surface which act as traps for the exciton.[23] Alkyl ligands that are used with

growth of NCs provide colloidal stability, but they can also lower QY. When used in optoelectronic applications such as LEDs and photovoltaics, the long alkyl chains should be removed as they impede electronic transport.[24,25] There are several ways to address these problems. One of the most popular methods is shell growth. Typically, layers of zinc selenide or zinc sulfide are grown on an InP core.[26,27] ZnS and ZnSe have wider band gaps than InP and a small lattice mismatch. While it is a popular method that produces quantum dots with high quantum yields, the synthesis can be hours or days long and requires a lot of material to grow the shells.[27,28] Another method is removal of the surface traps through post-synthetic etching or ligand removal. As shown in the literature, hydrofluoric acid (HF) is very effective at improving quantum yields by eliminating dangling phosphorous bonds and long alkyl ligands.[29,30] HF, however, is extremely dangerous; it is reported to cause severe respiratory irritation, edema, and hemorrhaging.[31,32] To avoid using more hazardous chemicals, we produce luminescent particles by using fluoride-containing ionic liquids and rapidly heating microwave-assisted synthesis.[33]

Microwaves are used in our everyday lives to conveniently heat up food. Similarly, they are useful tools in chemistry, because they allow for direct heating of polar materials with good loss tangent as they dissipate heat quickly.[34] There are two types of heating that can occur: dipolar polarization or ionic conduction.[35] During dipolar polarization, the dipoles of molecules will align or reverse align with the microwave pulses. By continually rotating with the pulses, they release their energy in the form of heat. For ionic conduction, ions or charged particles have increased electric fields and displacement of charges in response to the microwave pulses. They release this excess energy in the form of heat. Reaction parameters such as temperature, power, ramp time, and holding time can also be more regulated than traditional convective heating methods. Microwave-assisted heating reduces time scales of reactions and greatly improves

heating rates.[35] This is possible through the design of closed microwave vessels, which allows for higher pressures. Solvents can be heated beyond their normal boiling point, higher temperatures can be reached under higher pressurized conditions, and reaction rates are increased. Our work is based on research by Strouse *et al.* on microwave synthesis of InP nanocrystals using ionic liquids with varying anions and cations to determine which can produce nanocrystals with the highest QY.[36] Based on their selection of ionic liquids, they deduced that 1-hexyl-3-methyl-imidazolium tetrafluoroborate produced the highest QY of 47%. Recently, our group obtained luminescent, tunable sizes of InP nanocrystals using the ionic liquid, 1-butyl-4-methylpyridinium tetrafluoroborate, and amines.[33] Sizes were tuned from 3.2 to 4.2 nm with quantum yields up to 30% in a single step.

In conjunction with our microwave-assisted synthesis of InP nanocrystals, in this thesis we use ionic liquids containing either BF_4^- or PF_6^- ions as the microwave absorbers and less hazardous source of fluoride than HF to passivate the nanocrystal surface. This is done via direct heating of reactants, the ionic liquid and InP precursor in decane, in a microwave reactor. Figure 3a compares the UV-Vis absorption and photoluminescence (PL) spectra for InP QDs with BF_4^- containing ionic liquids at different microwave set-temperatures.[37] When temperature increases, size increases and the absorption and PL peaks shift to longer wavelengths. Figure 3b compares InP QDs prepared with and without BF_4^--containing ionic liquid. BF_4^- containing ionic liquid, such as 1-butyl-4-methylpyridinium tetrafluoroborate (BMPy BF_4), assists with the production of luminescent InP in a one-step reaction, nullifying the need for acquiring luminosity through post-synthetic modification. As seen in the absorption of the ionic liquid without BF_4^- or PF_6^-, 1-butyl-3-methylimidazolium *bis*(trifluoromethane)sulfonimide (BMIm TFSI), QDs form however, they do not luminesce, thus supporting the necessity of BF_4^- or PF_6^- containing ionic liquids for

surface passivation and increased luminescence.

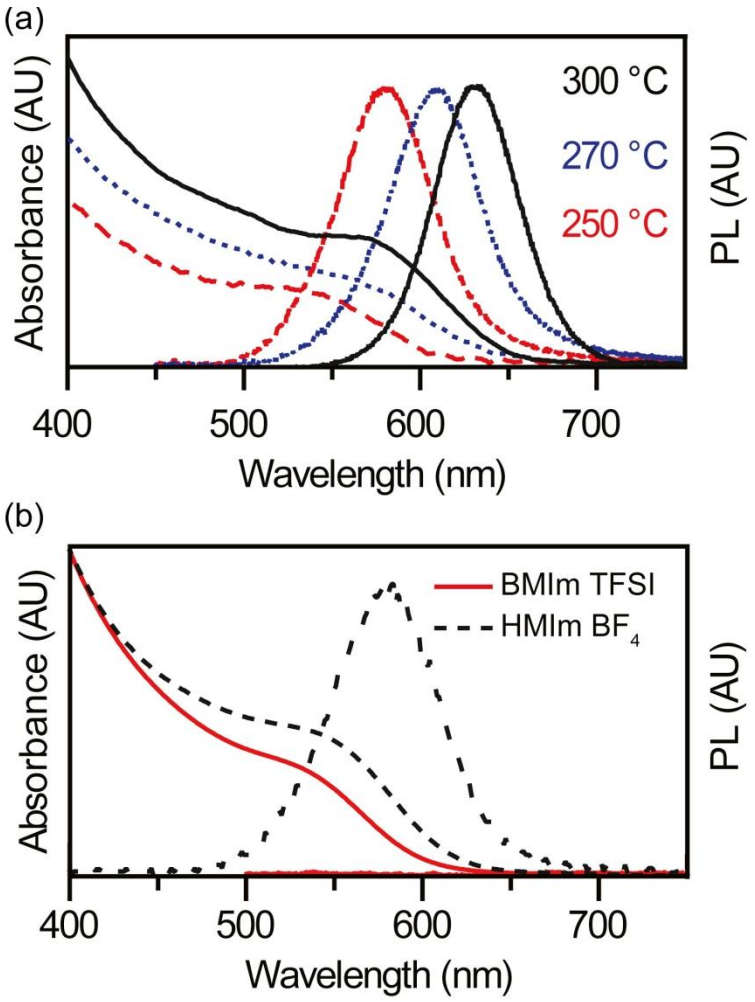

Figure 3. Absorption and photoluminescence spectra of InP QDs prepared in a microwave reactor with ILs at 800 W set power. (a) QDs size increases as temperature increases from 250-300 °C when synthesized with BF_4^- or PF_6-containing ILs. (b) QDs prepared at 280 °C with two types of ILs both have absorption features. BMIm TFSI, which has no BF_4^- or PF_6^-, does not produce luminescent QDs.[37]

This thesis uses the ionic liquid, 1-butyl-3-methylimidazolium tetrafluoroborate (BMIm BF_4), and the procedure is adapted from Strouse et al.[36] One of our goals is to determine the effect of different ratios of a separate-source precursor to ionic liquid (IL) on the size, size-distribution and quantum yield. We hypothesize that increasing amounts of IL result in smaller nanocrystals due to fluoride release and etching of the nanocrystals.

We also examine the MSC precursor to determine if the MSC is more stable and reproducible than a separate-source precursor. By using single-source precursors along with microwave-assisted ionic liquid synthesis, luminescent InP nanocrystals can be produced without using hazardous materials such as HF, or long procedures such as shell growth. We hypothesize that a combination of these reactants assist with luminescence and surface passivation by forming $[BF_n(O_2CR)_{4-n}]^-$ species with native ligands, based on work done by Helms *et al.*[38] When using the MSCs with ionic liquids to synthesize InP NCs, we hypothesize that the NCs produced will have a more narrow size-distribution and higher luminescence. Similar microwave reactions performed with an IL with a different anion, hexafluorophosphate. We synthesize luminescent InP NCs by heating the MSC precursor with ionic liquid in microwave reactor without further post-synthetic steps to achieve luminescent InP NCs.

Conducting these reactions in a microwave reactor provides many advantages, however, there are more factors to account for, such as interactions between the ionic liquid and microwave pulses. Ligand stripping and ligand exchange are another method to analyze native surface ligands. During these processes, the native surface ligands are displaced or replaced with other ions to stabilize the nanocrystal surface. In Chapter 3, we discuss the use of BF_3 in DMF as a Lewis acid source to displace the native carboxylate ligand.[38] Preliminary studies on the surface characterization of InP NCs and ligand exchange/stripping reactions were conducted to

determine what compounds were on the surface. Gaining understanding of the surface chemistry and etching mechanism is necessary to forming better syntheses and therefore better nanocrystals.

1.5 References

(1) Brus, L. E. A Simple Model for the Ionization Potential, Electron Affinity, and Aqueous Redox Potentials of Small Semiconductor Crystallites. *J. Chem. Phys.* **1983**, *79* (11), 5566–5571.

(2) Steckel, J. S.; Ho, J.; Hamilton, C.; Xi, J.; Breen, C.; Liu, W.; Allen, P.; Coe-Sullivan, S. Quantum Dots: The Ultimate down-Conversion Material for LCD Displays: Quantum Dot Enabled LCD Displays. *J. Soc. Inf. Disp.* **2015**, *23* (7), 294–305.

(3) Green, M. A.; Hishikawa, Y.; Warta, W.; Dunlop, E. D.; Levi, D. H.; Hohl-Ebinger, J.; Ho-Baillie, A. W. H. Solar Cell Efficiency Tables (Version 50). *Prog. Photovolt. Res. Appl.* **2017**, *25* (7), 668–676.

(4) Vaisman, M.; Fan, S.; Nay Yaung, K.; Perl, E.; Martín-Martín, D.; Yu, Z. J.; Leilaeioun, M.; Holman, Z. C.; Lee, M. L. 15.3%-Efficient GaAsP Solar Cells on GaP/Si Templates. *ACS Energy Lett.* **2017**, *2* (8), 1911–1918.

(5) Smith, B. R.; Gambhir, S. S. Nanomaterials for In Vivo Imaging. *Chem. Rev.* **2017**, *117* (3), 901–986.

(6) Zhang, J.; Wang, J.; Yan, T.; Peng, Y.; Xu, D.; Deng, D. InP/ZnSe/ZnS Quantum Dots with Strong Dual Emissions: Visible Excitonic Emission and near-Infrared Surface Defect Emission and Their Application in in Vitro and in Vivo Bioimaging. *J. Mater. Chem. B* **2017**, *5* (41), 8152–8160.

(7) Wu, Y.-Z.; Sun, J.; Zhang, Y.; Pu, M.; Zhang, G.; He, N.; Zeng, X. Effective Integration of Targeted Tumor Imaging and Therapy Using Functionalized InP QDs with VEGFR2 Monoclonal Antibody and MiR-92a Inhibitor. *ACS Appl. Mater. Interfaces* **2017**, *9* (15), 13068–13078.

(8) Talapin, D. V.; Steckel, J. Quantum Dot Light-Emitting Devices. *MRS Bull.* **2013**, *38* (9), 685–691.

(9) Reiss, P.; Carrière, M.; Lincheneau, C.; Vaure, L.; Tamang, S. Synthesis of Semiconductor Nanocrystals, Focusing on Nontoxic and Earth-Abundant Materials. *Chem. Rev.* **2016**, *116* (18), 10731–10819.

(10) Tamang, S.; Lincheneau, C.; Hermans, Y.; Jeong, S.; Reiss, P. Chemistry of InP Nanocrystal Syntheses. *Chem. Mater.* **2016**, *28* (8), 2491–2506.

(11) Smith, A. M.; Nie, S. Semiconductor Nanocrystals: Structure, Properties, and Band Gap Engineering. *Acc. Chem. Res.* **2010**, *43* (2), 190–200.

(12) Donegá, C. de M. Synthesis and Properties of Colloidal Heteronanocrystals. *Chem. Soc. Rev.* **2011**, *40* (3), 1512–1546.

(13) Reiss, P.; Carrière, M.; Lincheneau, C.; Vaure, L.; Tamang, S. Synthesis of Semiconductor Nanocrystals, Focusing on Nontoxic and Earth-Abundant Materials. *Chem. Rev.* **2016**, *116* (18), 10731–10819.

(14) Nightingale, A. M.; deMello, J. C. Improving the Ensemble Optical Properties of InP Quantum Dots by Indium Precursor Modification. *J. Mater. Chem. C* **2016**, *4* (36), 8454–8458.

(15) Boles, M. A.; Ling, D.; Hyeon, T.; Talapin, D. V. The Surface Science of Nanocrystals. *Nat. Mater.* **2016**, *15*, 141.

(16) Cossairt, B. M. Shining Light on Indium Phosphide Quantum Dots: Understanding the Interplay among Precursor Conversion, Nucleation, and Growth. *Chem. Mater.* **2016**, *28* (20), 7181–7189.

(17) Gary, D. C.; Terban, M. W.; Billinge, S. J. L.; Cossairt, B. M. Two-Step Nucleation and Growth of InP Quantum Dots via Magic-Sized Cluster Intermediates. *Chem. Mater.* **2015**, *27* (4), 1432–1441.

(18) Malik, M. A.; Afzaal, M.; O'Brien, P. Precursor Chemistry for Main Group Elements in Semiconducting Materials. *Chem. Rev.* **2010**, *110* (7), 4417–4446.

(19) Xie, R.; Li, Z.; Peng, X. Nucleation Kinetics vs Chemical Kinetics in the Initial Formation of Semiconductor Nanocrystals. *J. Am. Chem. Soc.* **2009**, *131* (42), 15457–15466.

(20) Yang, X.; Zhao, D.; Leck, K. S.; Tan, S. T.; Tang, Y. X.; Zhao, J.; Demir, H. V.; Sun, X. W. Full Visible Range Covering InP/ZnS Nanocrystals with High Photometric Performance and Their Application to White Quantum Dot Light-Emitting Diodes. *Adv. Mater.* **2012**, *24* (30), 4180–4185.

(21) Gary, D. C.; Flowers, S. E.; Kaminsky, W.; Petrone, A.; Li, X.; Cossairt, B. M. Single-Crystal and Electronic Structure of a 1.3 Nm Indium Phosphide Nanocluster. *J. Am. Chem. Soc.* **2016**, *138* (5), 1510–1513.

(22) Kwon, S. G.; Hyeon, T. Formation Mechanisms of Uniform Nanocrystals via Hot-Injection and Heat-Up Methods. *Small* **2011**, *7* (19), 2685–2702.

(23) Fu, H.; Zunger, A. InP Quantum Dots: Electronic Structure, Surface Effects, and the Redshifted Emission. *Phys. Rev. B* **1997**, *56* (3), 1496–1508.

(24) Mnoyan, A. N.; Kirakosyan, A. G.; Kim, H.; Jang, H. S.; Jeon, D. Y. Electrostatic Stabilized InP Colloidal Quantum Dots with High Photoluminescence Efficiency http://pubs.acs.org/doi/abs/10.1021/acs.langmuir.5b00847 (accessed Sep 28, 2017).

(25) Nag, A.; Kovalenko, M. V.; Lee, J.-S.; Liu, W.; Spokoyny, B.; Talapin, D. V. Metal-Free Inorganic Ligands for Colloidal Nanocrystals: S2–, HS–, Se2–, HSe–, Te2–, HTe–, TeS32–, OH–, and NH2– as Surface Ligands. *J. Am. Chem. Soc.* **2011**, *133* (27), 10612–10620.

(26) Reiss, P.; Protière, M.; Li, L. Core/Shell Semiconductor Nanocrystals. *Small* **2009**, *5* (2), 154–168.

(27) Altıntas, Y.; Talpur, M. Y.; Ünlü, M.; Mutlugün, E. Highly Efficient Cd-Free Alloyed Core/Shell Quantum Dots with Optimized Precursor Concentrations. *J. Phys. Chem. C* **2016**, *120* (14), 7885–7892.

(28) Bang, E.; Choi, Y.; Cho, J.; Suh, Y.-H.; Ban, H. W.; Son, J. S.; Park, J. Large-Scale Synthesis of Highly Luminescent InP@ZnS Quantum Dots Using Elemental Phosphorus Precursor. *Chem. Mater.* **2017**, *29* (10), 4236–4243.

(29) Talapin, D. V.; Gaponik, N.; Borchert, H.; Rogach, A. L.; Haase, M.; Weller, H. Etching of Colloidal InP Nanocrystals with Fluorides: Photochemical Nature of the Process Resulting in High Photoluminescence Efficiency. *J. Phys. Chem. B* **2002**, *106* (49), 12659–12663.

(30) Adam, S.; Talapin, D. V.; Borchert, H.; Lobo, A.; McGinley, C.; de Castro, A. R. B.; Haase, M.; Weller, H.; Möller, T. The Effect of Nanocrystal Surface Structure on the Luminescence Properties: Photoemission Study of HF-Etched InP Nanocrystals. *J. Chem. Phys.* **2005**, *123* (8), 084706.

(31) Levels, N. R. C. (US) S. on A. E. G. *Hydrogen Fluoride:Acute Exposure Guideline Levels*; National Academies Press (US), 2004.

(32) MacKinnon, M. A. Hydrofluoric Acid Burns. *Dermatol. Clin.* **1988**, *6* (1), 67–74.

(33) Siramdas, R.; McLaurin, E. J. InP Nanocrystals with Color-Tunable Luminescence by Microwave-Assisted Ionic-Liquid Etching. *Chem. Mater.* **2017**, *29* (5), 2101–2109.

(34) Gabriel, C.; Gabriel, S.; Grant, E. H.; Grant, E. H.; Halstead, B. S. J.; Mingos, D. M. P. Dielectric Parameters Relevant to Microwave Dielectric Heating. *Chem. Soc. Rev.* **1998**, *27* (3), 213–224.

(35) Zhu, Y.-J.; Chen, F. Microwave-Assisted Preparation of Inorganic Nanostructures in Liquid Phase. *Chem. Rev.* **2014**, *114* (12), 6462–6555.

(36) Lovingood, D. D.; Strouse, G. F. Microwave Induced In-Situ Active Ion Etching of Growing InP Nanocrystals. *Nano Lett.* **2008**, *8* (10), 3394–3397.

(37) Lee, S. K.; McLaurin, E. J. Recent Advances in Colloidal Indium Phosphide Quantum Dot Production. *Curr. Opin. Green Sustain. Chem.*

(38) Doris, S. E.; Lynch, J. J.; Li, C.; Wills, A. W.; Urban, J. J.; Helms, B. A. Mechanistic Insight into the Formation of Cationic Naked Nanocrystals Generated under Equilibrium Control. *J. Am. Chem. Soc.* **2014**, *136* (44), 15702–15710.

Chapter 2 - Effect of Varying Ionic Liquid Ratios on Indium Phosphide

2.1 Introduction

As mentioned in the previous section, one way to modify the surface is by etching the surface with fluoride and estudies used HF as an etchant.[1–4] Surface passivation occurs when ligands bind to dangling bonds, the energy of the surface and trap states are shifted away from the HOMO-LUMO gap and nonradiative relaxation is prevented. The quantum yield (QY) increases dramatically, and it is theorized that surface vacancies were removed with fluoride.[1,5] Upon using this method, dangling bonds or unsatisfied valencies on the nanocrystal surface are eliminated.[1,6] This lessens the possibility of surface traps that can encapture excitons and result in broad photoluminescence. HF, however, is very deleterious to our health and other alternatives should be pursued.[7] Core/shell growth is another method of surface passivation and passivates by growing layers of another material onto the core of the nanocrystal.[8] Ideally, if there is lattice mismatch between the two materials, it should be as minimal as possible to reduce the possibility of nonradiative recombination within the material. The nanocrystal's native ligands can also be exchanged with different ligands, affecting the nanocrystal solubility in polar or nonpolar solvents.[9–12] Within the last 10 years, ionic liquids (IL) have been employed for nanocrystal synthesis: the Strouse group has done extensive studies on multiple types of fluoride-containing ionic liquids in microwave reactions to examine their effect on quantum yield and size distribution.[6,13,14]

Ionic liquids are thought to etch the surface of NCs, thereby eradicating phosphorous dangling bonds and leading to higher quantum yields. Upon reaching an ionic liquid's decomposition temperature, fluoride ions are released from the anion, and small amounts of HF

can be produced *in situ*.[1,2] Based on studies by Strouse and co-workers, for most of the ionic liquids they tested the 1:10 ratio of precursor to ionic liquid resulted in the highest QY.[15] We use the 1-butyl-3-methylimidazolium tetrafluoroborate (BMIm BF_4) ionic liquid, because it is cheap and widely available. Our goal is to determine if larger volumes of ionic liquid will produce more highly luminescent nanocrystals. The ionic liquid was also not used by the Strouse group. Our InP precursor is in decane as our high boiling nonpolar solvent, which is transparent to microwaves. All of the reactions are done in a Pyrex glass vessel that is transparent to microwaves and allows for direct heating of precursors. We hypothesized that increasing the concentration of ionic liquid results in a more narrow-size distribution. With more ionic liquid, more fluoride ions would be released, surface defects would be passivated, thus increasing the quantum yield.

2.2 Results and Discussion

The ratio between precursor and ionic liquid was varied to determine if the concentration of ionic liquid had a direct effect on the absorbance and photoluminescence of nanocrystals. A separate-source In^{3+} and P^{3-} precursor and ionic liquid combined in a microwave reactor to produce indium phosphide nanocrystals. As the concentration of ionic liquid increased, the reaction heated much more quickly. Heating too quickly during nanocrystal growth can lead to a broader size distribution and broader absorbance.[16] Figure 4 below shows the amount of ionic liquid that is in a 1:10 reaction. Reactions conducted for different ratios of precursor to ionic liquid were 1:1, 1:10, 1:50, and 1:75. After the microwave synthesis, the nanocrystals were purified. The purification procedure is shown in Figure 5. Some nanocrystals were left in the supernatant, so the first supernatant of each sample's purification step was saved for analysis.

The purification process could be improved to better isolate the nanocrystals perhaps by using size-selective precipitation. Figure 6 shows the absorption and photoluminescence spectra of InP NCs for each ratio.

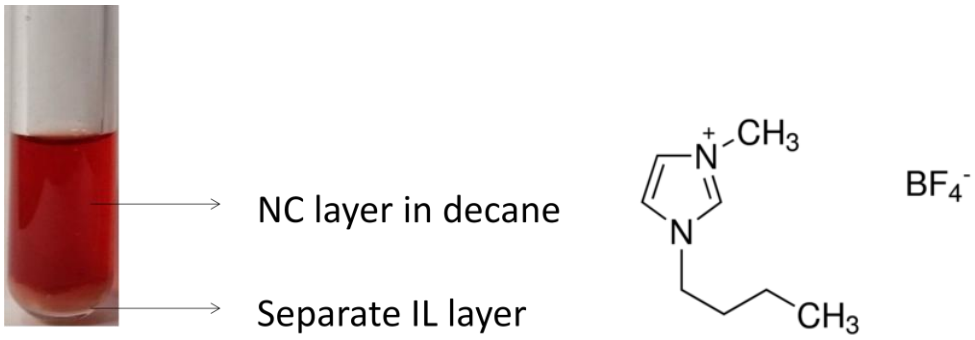

Figure 4. Microwave vial layered contents. The nanocrystal layer is in nonpolar decane solvent. The polar ionic liquid layer is a separate layer at the bottom. The structure shown is the ionic liquid, BMIm BF_4.

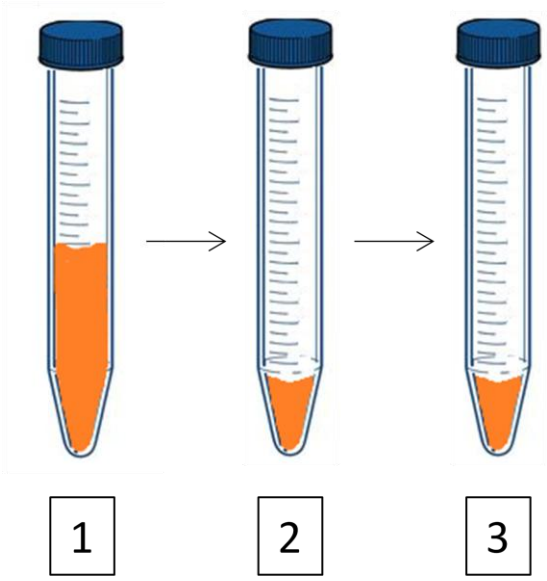

Figure 5. The purification procedure for InP NCs produced after a microwave reaction.

1) The nanocrystals were separated from the ionic liquid layer, precipitated with acetone, and centrifuged. The supernatant was decanted and saved for analysis.

2) The remaining nanocrystals were resuspended in a minimal amount of toluene, precipitated with acetone, and centrifuged. The supernatant was decanted again and discarded. The resuspension and precipitation procedure was repeated again.

3) The nanocrystals were resuspended in a minimal amount of toluene and stored in a glass vial.

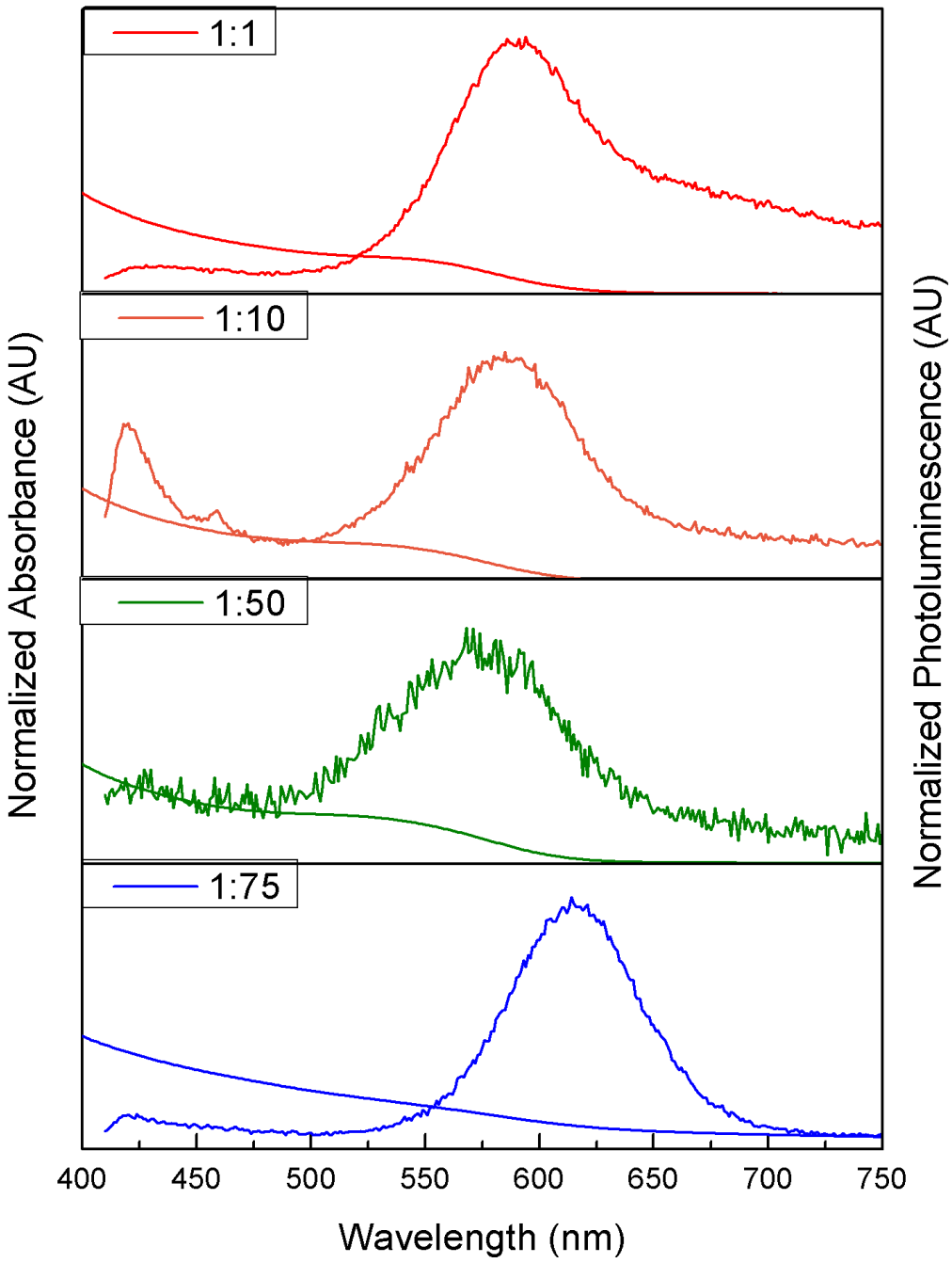

Figure 6. Absorbance and photoluminescence of nanocrystals produced with indium phosphide precursor and varying ratios of ionic liquid.

When examining the absorption features for the 1:1, 1:10, and 1:50 ratios, they shift to lower wavelengths from 540 to 520 nm, and the photoluminescence peak shifts from 594 to 568 nm, indicating a decrease in nanocrystal size. The photoluminescence for the 1:1 ratio has a shoulder at higher wavelengths, meaning that there are still traps on the surface from prevalent phosphorous dangling bonds. The photoluminescence for the 1:10 ratio has some insignificant emission at 425 nm that is due to instrument error. As the ionic liquid ratio increases to 1:75, there is a broad absorption feature. The photoluminescence for 1:75 is 614 nm. The intensity decreases greatly as well, possibly due to digestion of the nanocrystals by the IL.

The quantum yields were measured for the purified nanocrystals and for the supernatant from the first purification step. For the 1:1 ratio, some samples had low QY, but the nanocrystals stayed in the supernatant of the first washing. There may not have been enough BF_4^- to be decomposed by the microwave and etch the nanocrystal surface. The supernatant for the 1:10 ratio had the highest quantum yield of 21%, then 1:50 supernatant at 18%. The appendix has quantum yields for all of the samples. For the 1:75, there may have been too much ionic liquid which too much fluoride ion and BF_3 from the BF_4^- ion, digesting some of the particles. Some of the 1:75 particles also settled to bottom of the vial. When experiments were repeated with higher IL amounts (1:50, 1:75 and 1:100), arcing in the microwave occurred occasionally due to interactions between the polar IL and microwaves and the reactions were stopped.

How quickly the precursor is used after it is synthesized can also affect the nanocrystal quality, as seen in Figure 7 and Figure 8. In Figure 7, when precursors that are made on different days are used to repeat experiments, the nanocrystals produced do not always have the same absorption and photoluminescence spectra. There are many variables associated with the precursor usage, possibly due to the storage of the precursor in solution form. The type of

precursor used and different variables associated with it will be discussed in Chapter 3. Because there is so much variability with nanocrystals produced with the red, separate-source precursor, we decided to use a more recently characterized precursor, the InP magic-sized cluster. The microwave reactor conditions can also affect the quality of NCs. Typically the microwave is preheated before conducting experiments. The time between preheating the microwave and performing the first microwave reaction as well as performing consecutive reactions affects the nanocrystals produced, as seen in the absorption Figure 8. These nanocrystals were produced using the same reaction conditions, however, the experiments were conducted one after another which could have affected the heating and nanocrystal growth.

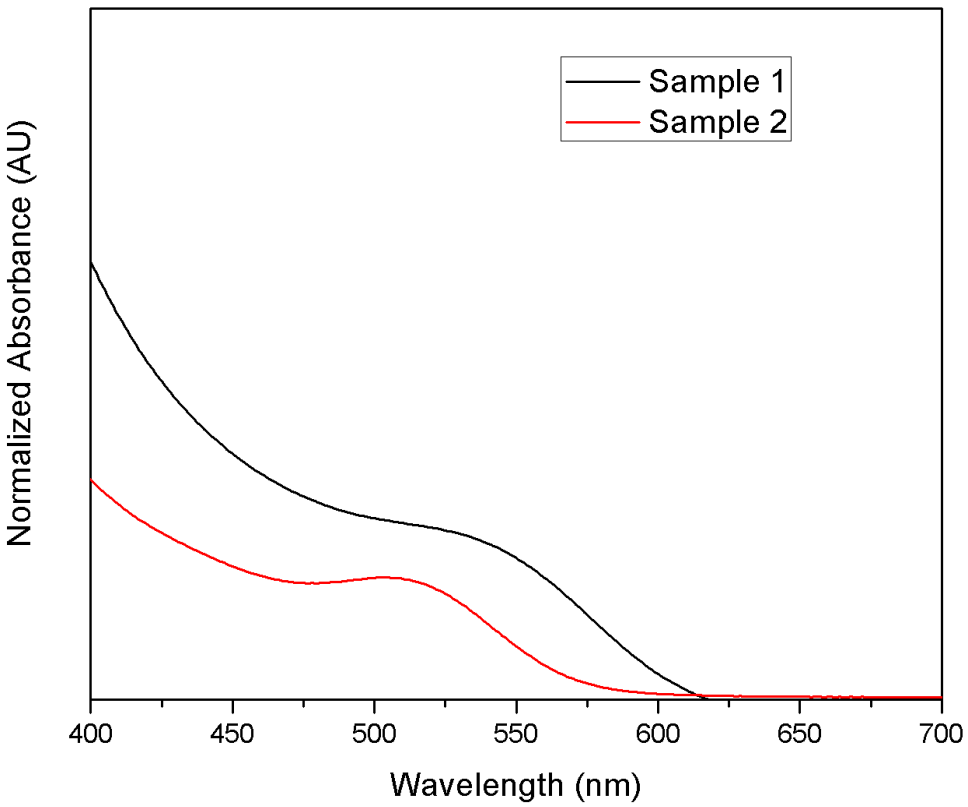

Figure 7. Normalized absorbance spectra of InP NCs. Both samples were 1:10 ratio of precursor to IL. NCs samples were made with different precursor batches on different days.

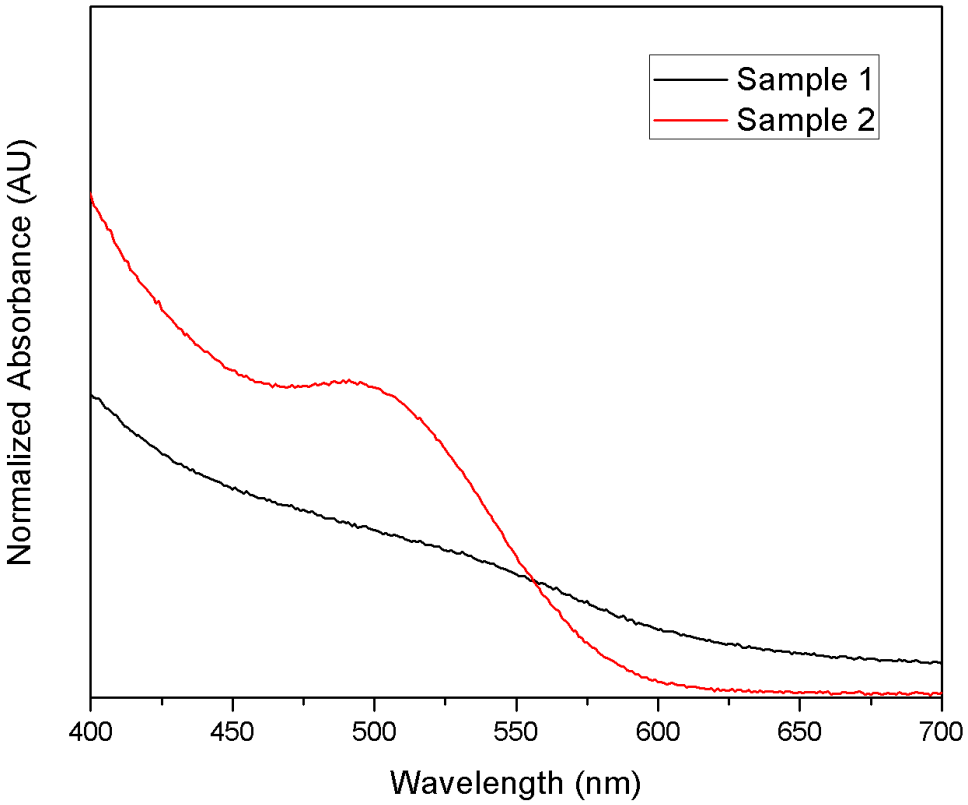

Figure 8. Normalized absorbance spectra of InP NCs. Both samples were 1:10 ratio of precursor to IL. The same precursor batch was used. The samples were made on the same day.

The microwave conveniently records parameters such as temperature, power, time, and pressure. This record keeping allows us to monitor the specific reaction conditions. Temperature vs. time and power vs. time plots are shown below in Figure 9**Error! Reference source not found.**.

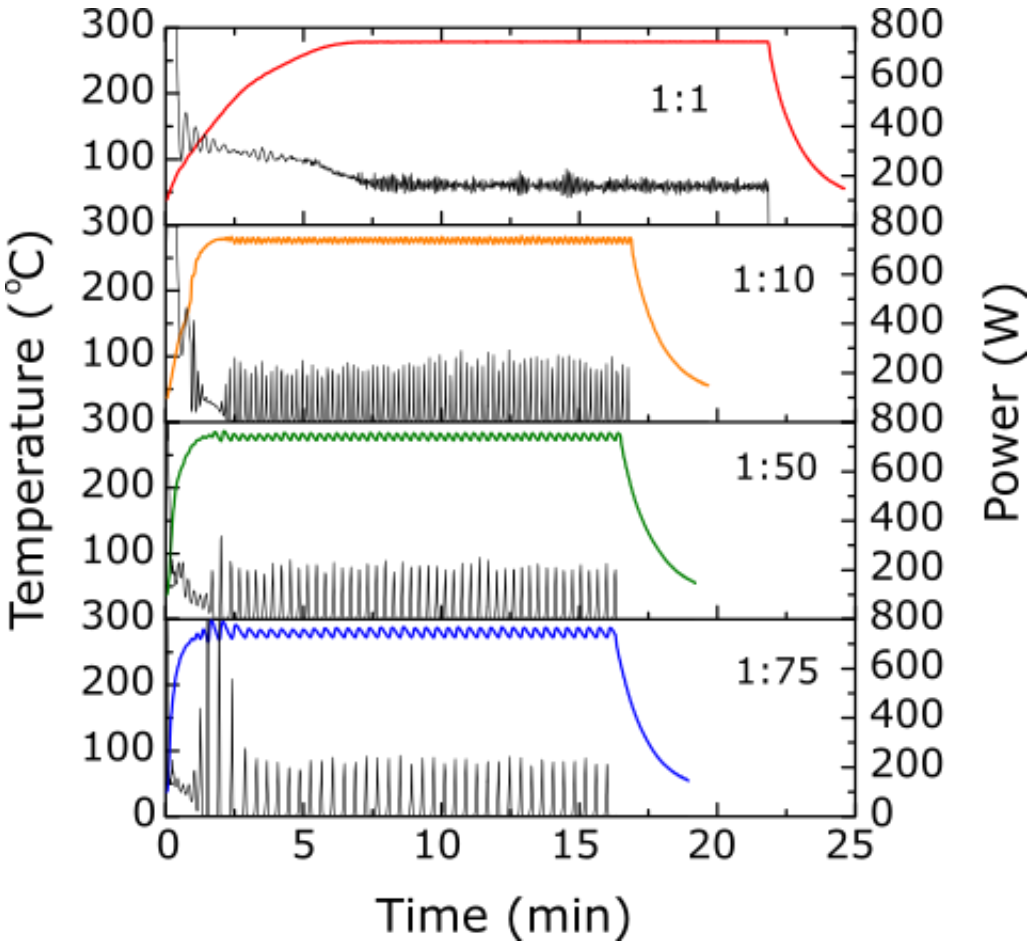

Figure 9. Microwave reactor settings for Temperature vs. Time and Power vs. Time for nanocrystals produced with indium phosphide precursor and varying ratios of ionic liquid. The colored lines correspond to temperature, and the black lines correspond to power.

The intensity and number of pulses is dependent on the volume of ionic liquid and power setting. When there is less ionic liquid, the reaction takes more time to reach the set temperature and the intensity of pulses of power is less, but there are more oscillations of pulses of power. When there is more ionic liquid, the reaction heats more quickly, and there are more intense pulses of

power, but there are less oscillations of pulses of power. As mentioned earlier, the microwaves interact strongly with polar materials. This is also dependent upon the volume of the materials. With larger volumes, the polar ionic liquid conducts a more intense electric field that causes arcing in the microwave as shown in Figure 10. As a safety precaution, the microwave stops the reaction. For the ratios 1:100, the reactions were conducted at a lower power of 300 W. Additional data for 1:100 is shown in the Appendix. With these experiments, we can begin to understand some of the factors and limitations of microwave reactions.

Figure 10. Microwave vial after 1:75 reaction in the microwave that resulted in arcing.

2.3 Conclusions

Overall, it is difficult to find a direct relationship between the moles of ionic liquid and moles of indium in the precursor because of how ionic liquids interact with microwaves. Microwave power can fluctuate depending on amount of polar material present, which affects reaction heating. This in turn affects the amount that ionic liquid is decomposed and quantum yield. The nanocrystal quality is dependent on when the precursor is made, when the precursor is used, amount of IL used, and when the reactions are conducted in the microwave. When doing consecutive reactions with higher amounts of IL, there was a higher likelihood of arcing and discontinuation of the reaction by the microwave. Similar to results by the Strouse group, the 1:10 ratio supernatant of InP precursor to ionic liquid, seems to be the optimal ratio for producing luminescent InP in a single reaction without shell growth or HF. The purification process could be improved in order to isolate more of the nanocrystals.

.

2.4 Experimental

Indium Palmitate (InPA)

This synthesis was adapted from a procedure by Strouse and co-workers and previously published by Siramdas and co-workers.[15,17] An air condenser and rubber septum was attached to a 100 mL two-neck round bottom flask (RBF). The apparatus was attached to a Schlenk line and placed under vacuum. The flask was then filled with N_2 and palmitic acid (0.605 g, 2.36 mmol) was added. The PA was heated in a 105 °C oil bath for 5-10 min, then cooled to room temperature under vacuum. The flask was placed under N_2, and indium acetate (0.207 g, 0.710 mmol) was added. The flask was evacuated again, and the solids were heated to 150 °C. The walls of the flask were heated repeatedly using a heat gun to dissolve any remaining solids until pressure reached baseline (1 hour). The flask was then cooled to room temperature under vacuum.

InP precursor

The flask containing solid InPA was brought into an inert atmosphere glovebox. Decane (47 mL) was added to the flask and allowed to stir until the solid was suspended in the solution (12 h). In the glovebox, *tris*(trimethylsilyl)phosphine (1.15 mL, 0.393 mmol) was diluted in decane (3 mL). This mixture was added to the InPA solution, which slowly turned orange (1-2 h). This InP precursor solution was then heated on a Schlenk line in an oil bath at 65 °C under N_2 until it turned optically clear (~10 min). The flask was stored in the glovebox for use in InP NC syntheses.

Microwave-Assisted InP NC Synthesis

Samples were prepared in a glovebox under inert atmosphere using capped 10 mL Pyrex glass microwave vessels with a stir bar. InP precursor (3 mL) and the ionic liquid, 1-methyl-3-butylimidazoliumtetrafluoroborate were added to a microwave vessel and capped. The ratio of In^{3+} in the precursor to IL varied. The vessel was brought out of the glovebox and quickly placed into the microwave reactor. The reaction proceeded in the microwave reactor using the parameters shown below in Table 1. Microwave synthesis conditions set for synthesis of InP nanocrystalsThe temperature is measured by using an infrared sensor that senses the temperature in the middle section of the reaction vial. This temperature measurement placement is specific to the Anton Paar Monowave 300.

	Temperature (°C)	**Time (min)**	**Power (W)**
Heat as fast as possible	280	As fast as possible	800
Holding time	-	15	800

Table 1. Microwave synthesis conditions set for synthesis of InP nanocrystals

After each microwave reaction was completed, it was cooled to 55 °C using compressed air. The decane/nanocrystal solution was isolated from the IL layer. The nanocrystal layer was precipitated using acetone and centrifuged at 5100 rpm for 5 minutes. The resulting solid was suspended in toluene and precipitated using acetone. This washing procedure was repeated 2 more times. Finally, the nanocrystals were stored in toluene.

The UV-Vis absorbance spectra were obtained using a Cary 5000 UV-Vis-NIR Spectrophotometer. Photoluminescence spectra and quantum yield measurements were recorded using a PTI Quanta Master 400 fluorometer. The quantum yields were calculated using either Fluorescein 0.1 N NaOH or Rhodamine B in or water as the reference. The equation below was used to calculate quantum yields.

$$\Phi_{sam} = \Phi_{ref}\left(\frac{A_{ref}}{A_{sam}}\right)\left(\frac{I_{sam}}{I_{ref}}\right)\left(\frac{\eta_{sam}}{\eta_{ref}}\right)^2$$

Φ_{ref} is the reference's emission quantum yield, A is the measured absorbance, I is the integrated photoluminescence, and η is the solvent's refractive index. Φ_{ref} was 0.95 for Fluorescein and 0.31 for Rhodamine B.

2.5 References

(1) Adam, S.; Talapin, D. V.; Borchert, H.; Lobo, A.; McGinley, C.; de Castro, A. R. B.; Haase, M.; Weller, H.; Möller, T. The Effect of Nanocrystal Surface Structure on the Luminescence Properties: Photoemission Study of HF-Etched InP Nanocrystals. *J. Chem. Phys.* **2005**, *123* (8), 084706.

(2) Talapin, D. V.; Gaponik, N.; Borchert, H.; Rogach, A. L.; Haase, M.; Weller, H. Etching of Colloidal InP Nanocrystals with Fluorides: Photochemical Nature of the Process Resulting in High Photoluminescence Efficiency. *J. Phys. Chem. B* **2002**, *106* (49), 12659–12663.

(3) Lester, S. D.; Kim, T. S.; Streetman, B. G. A Proposed Mechanism for Radiative Recombination through Surface States on InP. *J. Appl. Phys.* **1987**, *62* (7), 2950–2954.

(4) Li, C.; Ando, M.; Murase, N. Facile Preparation of Highly Luminescent InP Nanocrystals by a Solvothermal Route. *Chem. Lett.* **2008**, *37* (8), 856–857.

(5) Mićić, O. I.; Sprague, J.; Lu, Z.; Nozik, A. J. Highly Efficient Band- edge Emission from InP Quantum Dots. *Appl. Phys. Lett.* **1996**, *68* (22), 3150–3152.

(6) Gerbec, J. A.; Magana, D.; Washington, A.; Strouse, G. F. Microwave-Enhanced Reaction Rates for Nanoparticle Synthesis. *J. Am. Chem. Soc.* **2005**, *127* (45), 15791–15800.

(7) Levels, N. R. C. (US) S. on A. E. G. *Hydrogen Fluoride:Acute Exposure Guideline Levels*; National Academies Press (US), 2004.

(8) Reiss, P.; Protière, M.; Li, L. Core/Shell Semiconductor Nanocrystals. *Small* **2009**, *5* (2), 154–168.

(9) Doris, S. E.; Lynch, J. J.; Li, C.; Wills, A. W.; Urban, J. J.; Helms, B. A. Mechanistic Insight into the Formation of Cationic Naked Nanocrystals Generated under Equilibrium Control. *J. Am. Chem. Soc.* **2014**, *136* (44), 15702–15710.

(10) Mnoyan, A. N.; Kirakosyan, A. G.; Kim, H.; Jang, H. S.; Jeon, D. Y. Electrostatic Stabilized InP Colloidal Quantum Dots with High Photoluminescence Efficiency *Langmuir*. **2015,** *31* (25), 7117-7121.

(11) Huang, J.; Liu, W.; Dolzhnikov, D. S.; Protesescu, L.; Kovalenko, M. V.; Koo, B.; Chattopadhyay, S.; Shenchenko, E. V.; Talapin, D. V. Surface Functionalization of Semiconductor and Oxide Nanocrystals with Small Inorganic Oxoanions (PO_4^{3-}, MoO_4^{2-}) and Polyoxometalate Ligands. *ACS Nano* **2014**, *8* (9), 9388–9402.

(12) Kim, K.; Yoo, D.; Choi, H.; Tamang, S.; Ko, J.-H.; Kim, S.; Kim, Y.-H.; Jeong, S. Halide–Amine Co-Passivated Indium Phosphide Colloidal Quantum Dots in Tetrahedral Shape. *Angew. Chem. Int. Ed.* **2016**, *55* (11), 3714–3718.

(13) Washington II, A. L.; Strouse, G. F. Microwave Synthesis of CdSe and CdTe Nanocrystals in Nonabsorbing Alkanes. *J. Am. Chem. Soc.* **2008**, *130* (28), 8916–8922.

(14) Ashley, B.; D. Lovingood, D.; Chiu, Y.-C.; Gao, H.; Owens, J.; F. Strouse, G. Specific Effects in Microwave Chemistry Explored through Reactor Vessel Design, Theory, and Spectroscopy. *Phys. Chem. Chem. Phys.* **2015**, *17* (41), 27317–27327.

(15) Lovingood, D. D.; Strouse, G. F. Microwave Induced In-Situ Active Ion Etching of Growing InP Nanocrystals. *Nano Lett.* **2008**, *8* (10), 3394–3397.

(16) Ramasamy, P.; Kim, N.; Kang, Y.-S.; Ramirez, O.; Lee, J.-S. Tunable, Bright, and Narrow-Band Luminescence from Colloidal Indium Phosphide Quantum Dots. *Chem. Mater.* **2017**, *29* (16), 6893–6899.

(17) Siramdas, R.; McLaurin, E. J. InP Nanocrystals with Color-Tunable Luminescence by Microwave-Assisted Ionic-Liquid Etching. *Chem. Mater.* **2017**, *29* (5), 2101–2109.

Chapter 3 - Luminescent Indium Phosphide Nanocrystals Using Magic-Sized Clusters and Ionic Liquids

3.1 Introduction

Many quantum dot applications require high quantum yields and narrow size distribution.[1,2] One way to address these requirements is to use an established precursor. Clusters are stable intermediates that typically have atomically precise structures. Recently, the structure of indium phosphide clusters have been established. Cossairt and co-workers first published the presence of an indium phosphide cluster in 2015, termed magic-sized clusters (MSC).[3] These clusters are 1.3 nm in diameter and have a solved crystal structure using carboxylate ligands.[4] A precursor that can be reliably and uniformly reproduced eliminates many variables that can lead to inconsistencies in surface and size of nanocrystals. By using MSCs as a single-source precursor and ionic liquids as an etchant to improve quantum yields, luminescent InP NCs can be synthesized.

In order to achieve higher quantum yields without shells or HF etching, the long alkyl ligands that are used to stabilize quantum dots during growth must be removed or passivated for use in applications such as solar cells and displays.[5,6] This is possible through shell growth or ligand exchange or etching.[7–10] Ionic liquids have also been shown to produce luminescent nanocrystals.[11,12] Fluoride-containing ionic liquids with anions, such as BF_4^- or PF_6^-, are thought to assist with surface passivation through ligand stripping or exchange.[13,14] In the past, harsh, irreversible strongly electrophilic reagents such as Meerwein's salt were used to remove ligands from the NC surface. While effective, it also resulted in cation desorption and unstable surfaces due to lack of stabilizing agents. Others have also used HF or H_2SO_4. Helms and co-workers used BF_3:EtO_2 to form Lewis acid-base adducts of BF_3 to undergo nanocrystal ligand stripping

with PbSe NCs.[1,2] The anionic compounds that were produced from the reaction between BF_3 and native ligands helped stabilize the nanocrystal surface, thus avoiding cation desorption and destabilization. Helms and co-workers confirm that BF_3 is forming an adduct with carboxylates removed from the surface. They also performed zeta-potential experiments on the PbSe NCs and determined that they had a positive surface charge, which indicated that anionic species were coordinating to a positively charged metal surface. Ligand stripping and ligand exchange can be a tool to examine ligands that were on the nanocrystal surface, by using NMR and IR to identify the byproducts and changes on the nanocrystal surface. Upon conducting a similar experiment with InP NCs, we produce luminescent, stable, and polar InP NCs.

We can examine the reaction byproducts from cluster and ionic liquid reactions to better understand how the mechanisms work. The goals of this project are:

- Examine reproducibility of InP MSCs
- Examine cluster stability in solution versus solid form
- Determine if luminescent InP NCs produced by microwave-assisted ionic liquid synthesis with clusters have more narrow size distribution than InP NCs synthesized with separate-source precursor that was used in the previous chapter
- Conduct preliminary ligand stripping experiments to determine surface compounds: are carboxylate byproducts or phosphorous-fluorine compounds produced? [11,13]

3.2 Results and Discussion

Magic-Sized Cluster

First, we synthesized MSCs based on the procedure by Cossairt and co-workers.[3] Upon injecting the phosphorous precursor at 110 °C, the cluster's first absorbance feature red shifts

until stabilization at 386 nm. While synthesizing MSCs, small differences in temperatures (106 - 113 °C) can result in absorbances that are broad or have different wavelengths. This may be due to difficulty in accurately measuring the temperature. Banin and coworkers also noticed the appearance of different InP clusters (365 nm, 386 nm, and 395 nm) at different temperatures.[15] We used a thermometer and temperature probe during the reaction. The temperature of an oil bath can be difficult to accurately measure using a standard thermometer. The temperature probe was used in the reaction flask to directly get temperature measurements. Figure 11 shows absorbance aliquots from two different experiments. For samples 1, at lower temperatures, below 110 °C, clusters grow to an absorbance of 365 nm. For sample 2, between 110-115 °C, clusters grow to approximately 386 nm. The absorption aliquots taken while the clusters were grown at approximately 110 °C are shown in Figure 12**Error! Reference source not found.**. The clusters are grown for approximately 50 minutes until they reach an absorbance of 386 nm. After the clusters were synthesized, they were purified using a combination of toluene and acetonitrile as the solvent and antisolvent, respectively. After the final purification, the clusters were resuspended in pentane and dried under evacuation.

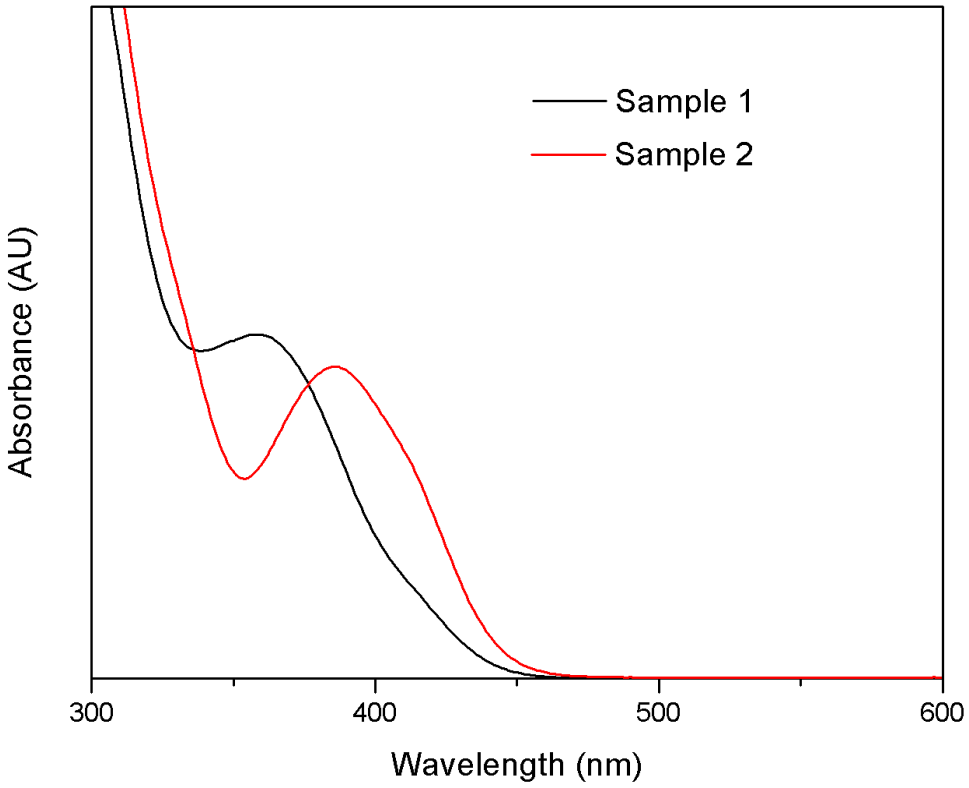

Figure 11. Absorbance aliquots from two different MSC experiments. Difficulty in controlling temperature may have resulted in synthesis of MSCs at two different sizes due to two different absorption features at 365 nm and 386 nm.

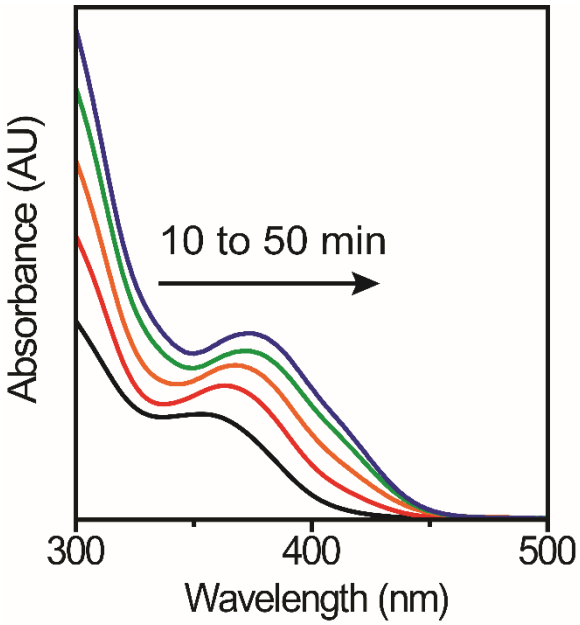

Figure 12. Absorbance of aliquots of clusters that were grown for approximately 50 minutes until their absorbance stabilized at 386 nm.

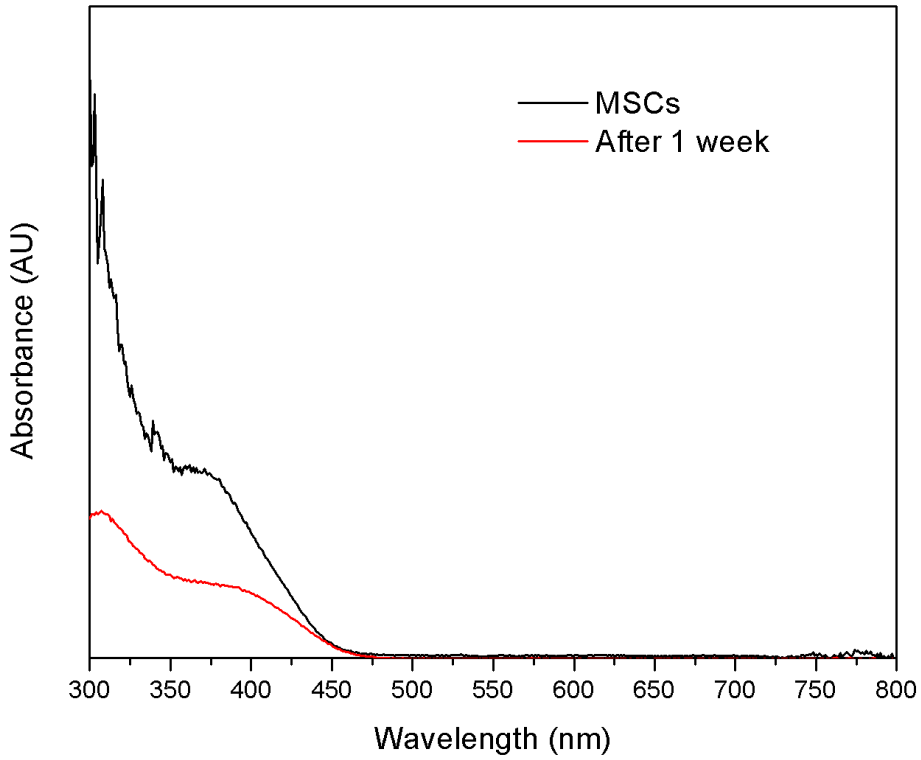

Figure 13. Absorption spectra of MSCs while stored in toluene: immediately after purification versus after one week of storage.

We compared the stability of the MSCs when stored over time in toluene and as a solid under inert atmosphere. The absorption spectra in Figure 14 shows broadening of the 386 nm absorption feature over time when the clusters are stored in toluene. The clusters are possibly becoming destabilized or aggregating. This may also indicate that the red, separate-source precursor used in previous syntheses may not be stable over a long period of time. When stored as a solid, as seen in Figure 14, the clusters retain their stability for longer. The absorption feature at 386 nm does not broaden as quickly.

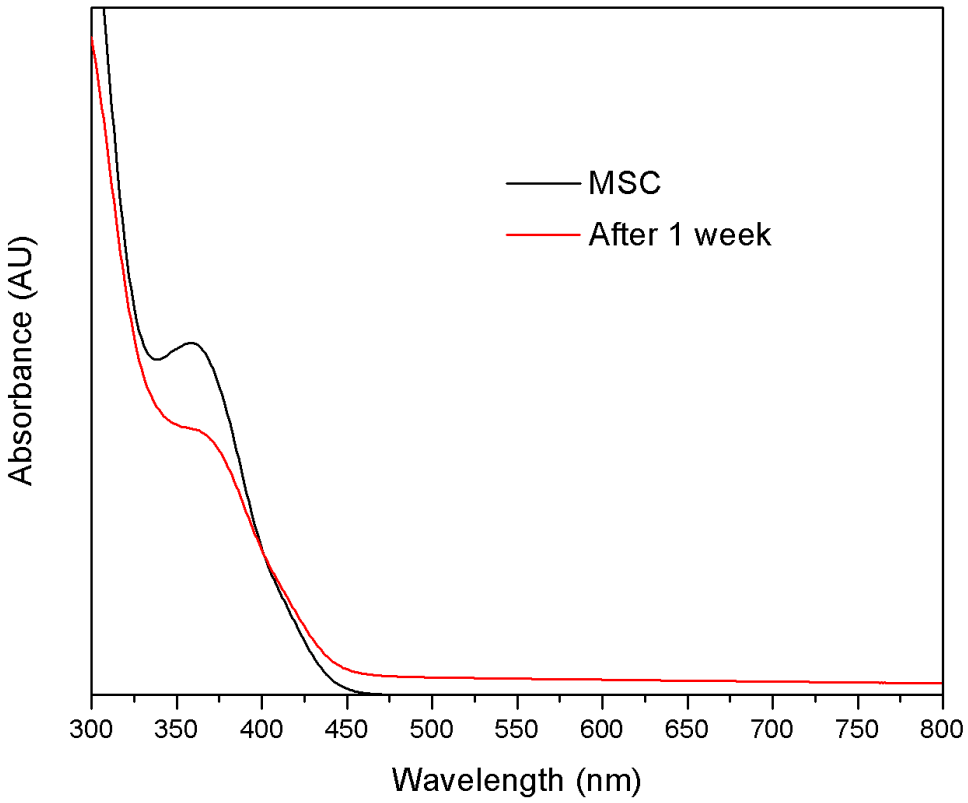

Figure 14. MSCs after purification versus storage as a solid after one week.

The ^{1}H NMR of the purified clusters shows slightly broadened myristate peaks indicating that there is myristate on the surface and most of the free myristate ligand has been removed from the sample. Free myristate appears as sharp peaks diffusing quickly off the nanocrystal surface. We also see leftover tristrimethylsilyl at 0.07 ppm, as shown in Figure 15**Error! Reference source not found.**. TMS-MA occurs at 0.26 ppm however, we do not see that peak.[16,17]

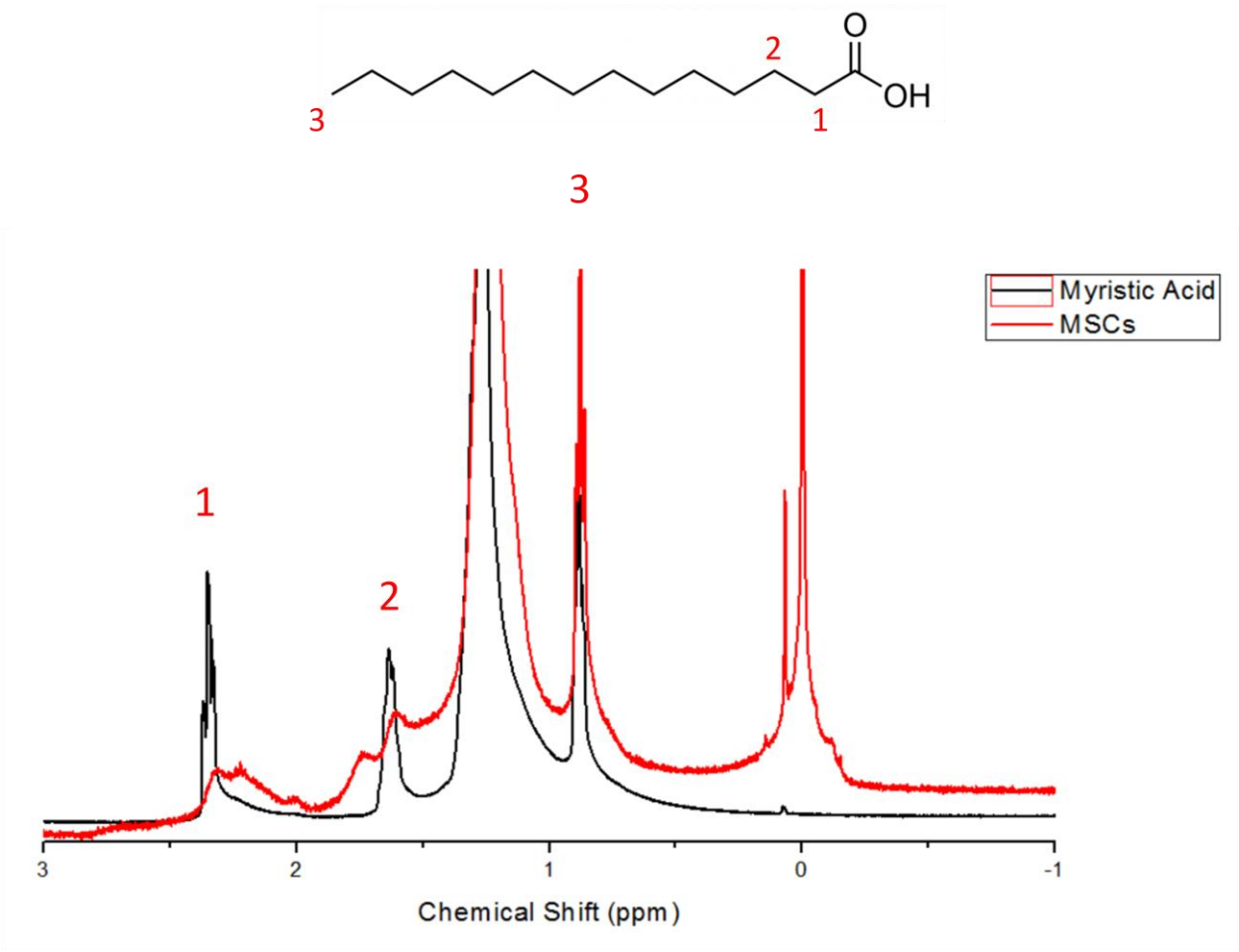

Figure 15. ^{1}H NMR of cluster compared to myristic acid. There are broadened myristate peaks and possible silyl groups at 0.07 ppm.

3.1 Characterization of Products after Microwave-Assisted Ionic Liquid Synthesis

The purified clusters were used as the InP precursor for nanocrystal synthesis. The microwave procedure was adapted from Strouse et al.[11] The solid MSC was resuspended in decane. It and the BMIm BF_4 ionic liquid were added to a Pyrex vessel, and the reaction was heated in a microwave reactor.

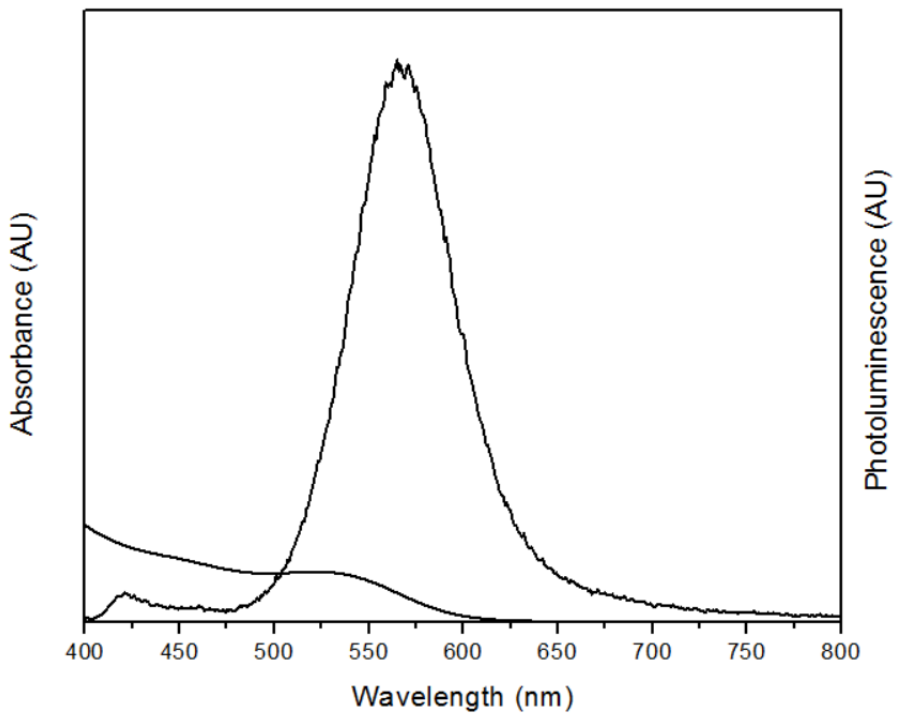

Figure 16. InP NCs synthesized using BMIm BF_4 in a microwave reactor.

After synthesizing the nanocrystals in the microwave reactor, the ionic liquid layer was separated from the decane layer. Each batch of nanocrystals was washed twice using toluene and acetone as the solvent and antisolvent. Figure 17 shows the absorption and photoluminescence of the NCs. Luminescent InP NCs can be produced without further post-synthetic steps.

We compared the NCs produced with the red, separate-source precursor and MSCs. The absorption spectra of the NCs are shown in Figure 18. The NCs produced using the MSCs have a sharper absorption peak, indicating a more narrow size distribution.

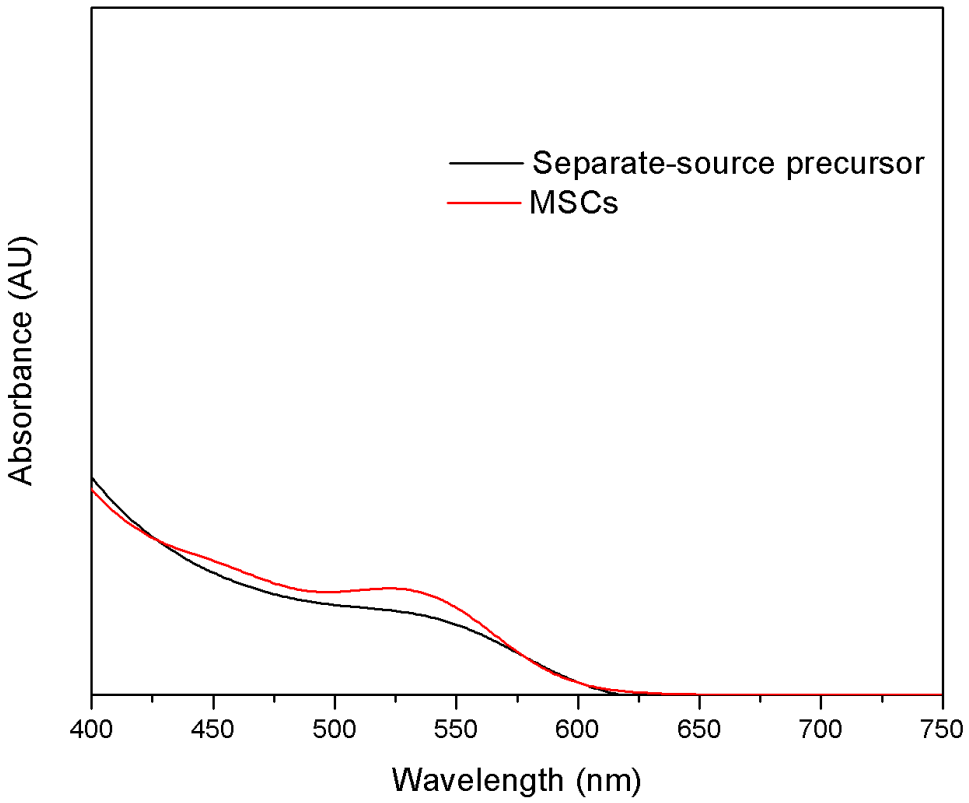

Figure 17. UV-vis absorption comparison between NCs produced by separate-source precursor and MSCs.

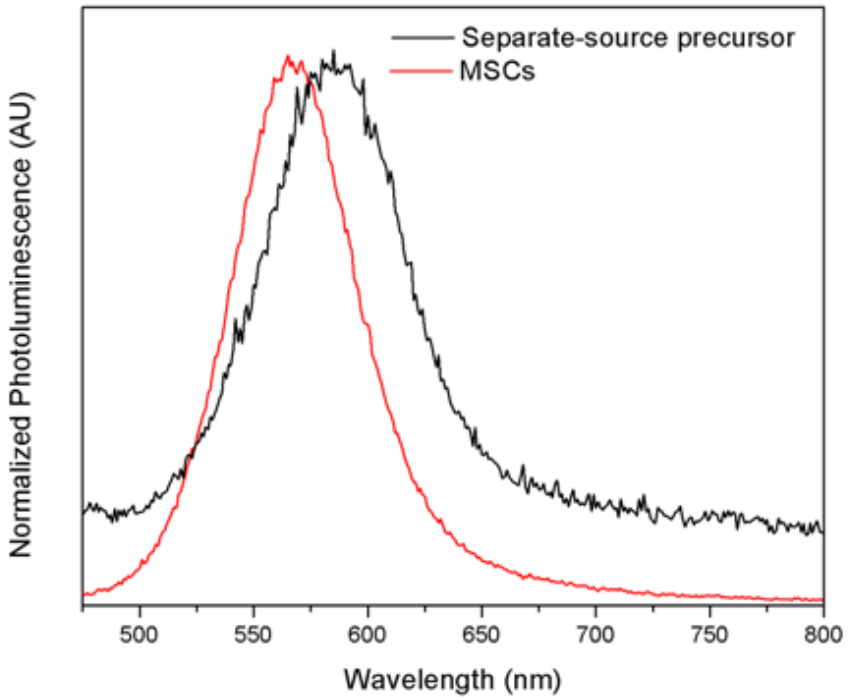

Figure 18. Photoluminescence plot of the NCs produced by separate-source precursor and MSCs.

When comparing the photoluminescence spectra of the NCs produced by separate-source precursor and MSCs, the NCs produced by the MSCs appear to have emission at lower wavelengths. The FWHM of the separate-source precursor = 65.7 eV and the MSCs = 66 eV. Based on the FWHM, the NCs produced by the two precursors do not differ greatly in size distribution, but more studies should be done to corroborate this.

The ^{1}H NMR of the clusters was compared to the NCs in Figure 19. After purification of NCs, there are still myristate ligands on the surface as indicated by the broadened peaks. The ionic liquid prior to and after microwave synthesis was examined as well using NMR. Any possible byproducts in the ionic liquid layer may provide clues about the etching mechanism as

there maybe compounds bonding to the ionic liquid.

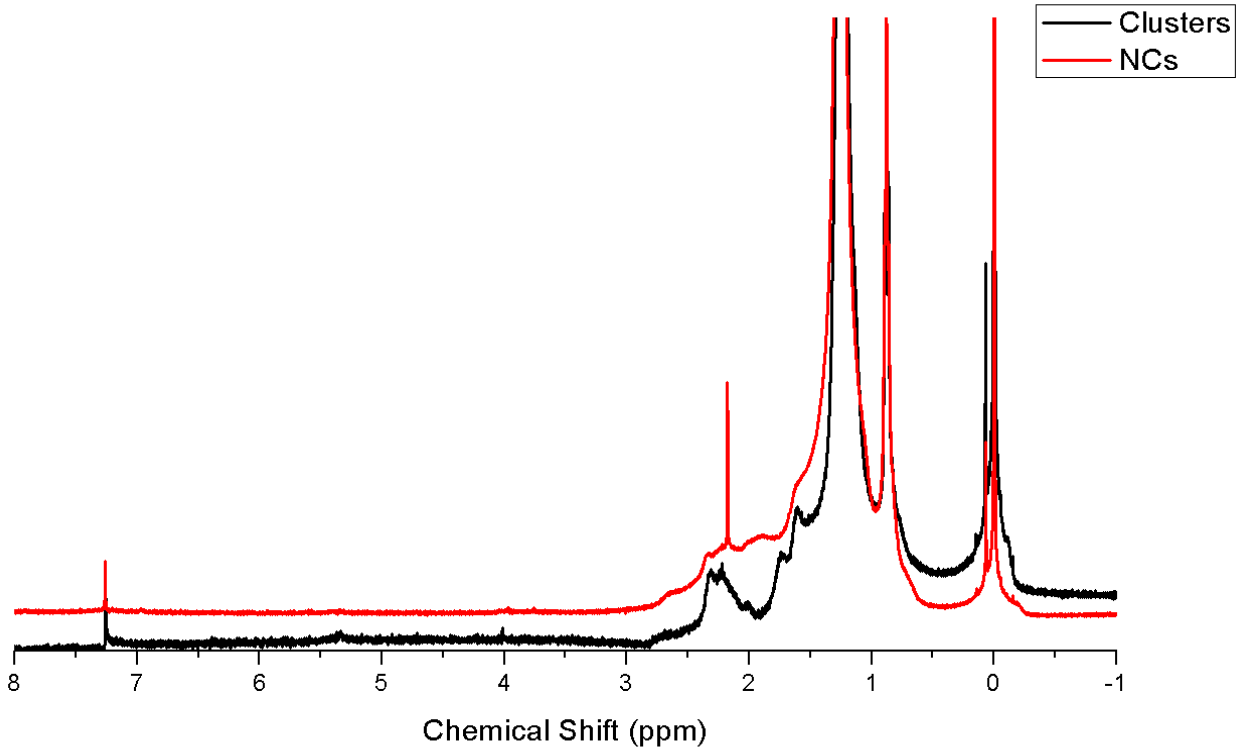

Figure 19. ^{1}H NMR of MSCs in comparison to InP NCs.

^{1}H NMR of the ionic liquid layer after microwave reactions was obtained and compared to unreacted ionic liquid as shown in Figure 20**Error! Reference source not found.** and the ^{19}F NMR is shown in Figure 21.

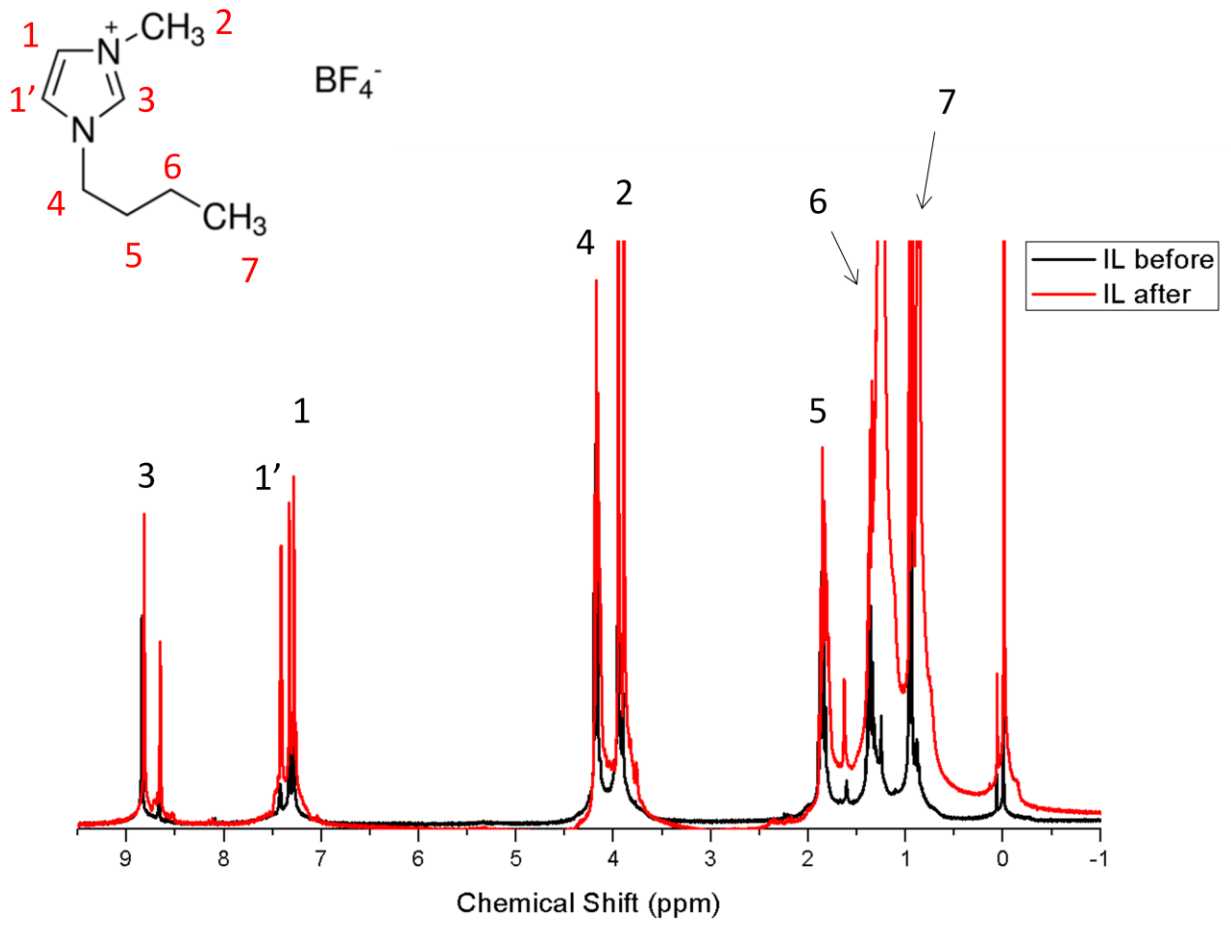

Figure 20 . ^{1}H NMR of BMIm BF_4 ionic liquid before and after microwave synthesis.

The ^{1}H NMR of BMIm BF_4 ionic liquid does not show much change in the cation before and after MW synthesis, except maybe some cation decomposition. None of the InP peaks correspond to protons on the NC surface, because they are not broadened. The peaks between 1 and 2 ppm could correspond to decomposed myristate. The peaks shift downfield slightly, possibly indicating the loss of the anion.

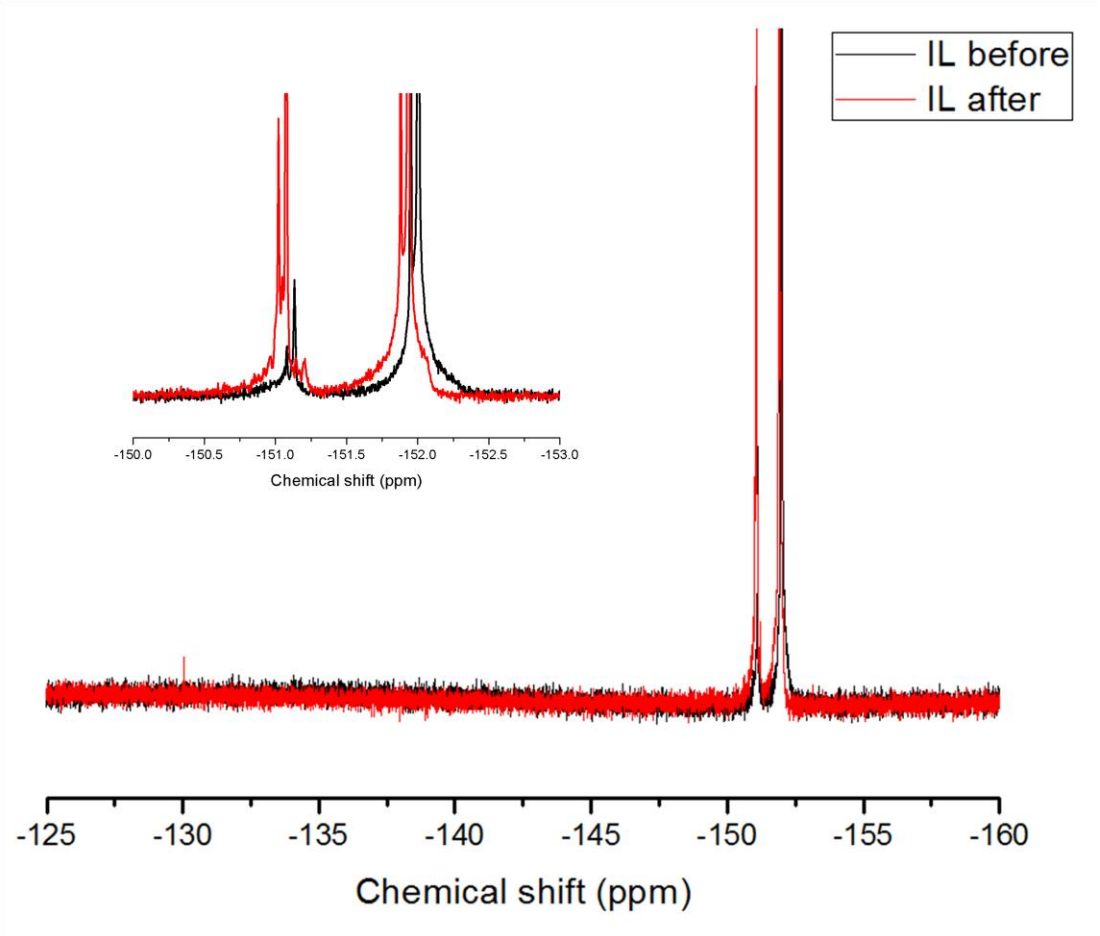

Figure 21. ^{19}F NMR of BMIm BF_4 before and after MW reaction. Inset: Zoomed in region of ^{19}F NMF of BMIm BF_4^- before and after MW reaction.

In the ^{19}F NMR of the IL before and after MW reaction, there are no other peaks to indicate the production of HF, which would be at 30 ppm. Upon zooming into the BF_4^- region, the peaks are shifted slightly after MW synthesis. There is BF_4^- at -152 ppm. The peaks are in a 1:4 ratio, and there are two different peaks in the bottom spectrum possibly due to the two different isotopes of boron. This peak shifts slightly after microwave reaction. NMRs of control experiments also show a BF_4^- peak in the same position. There is no ^{19}F NMR spectra of the nanocrystals, because no fluorine species were detected on the nanocrystal surface.

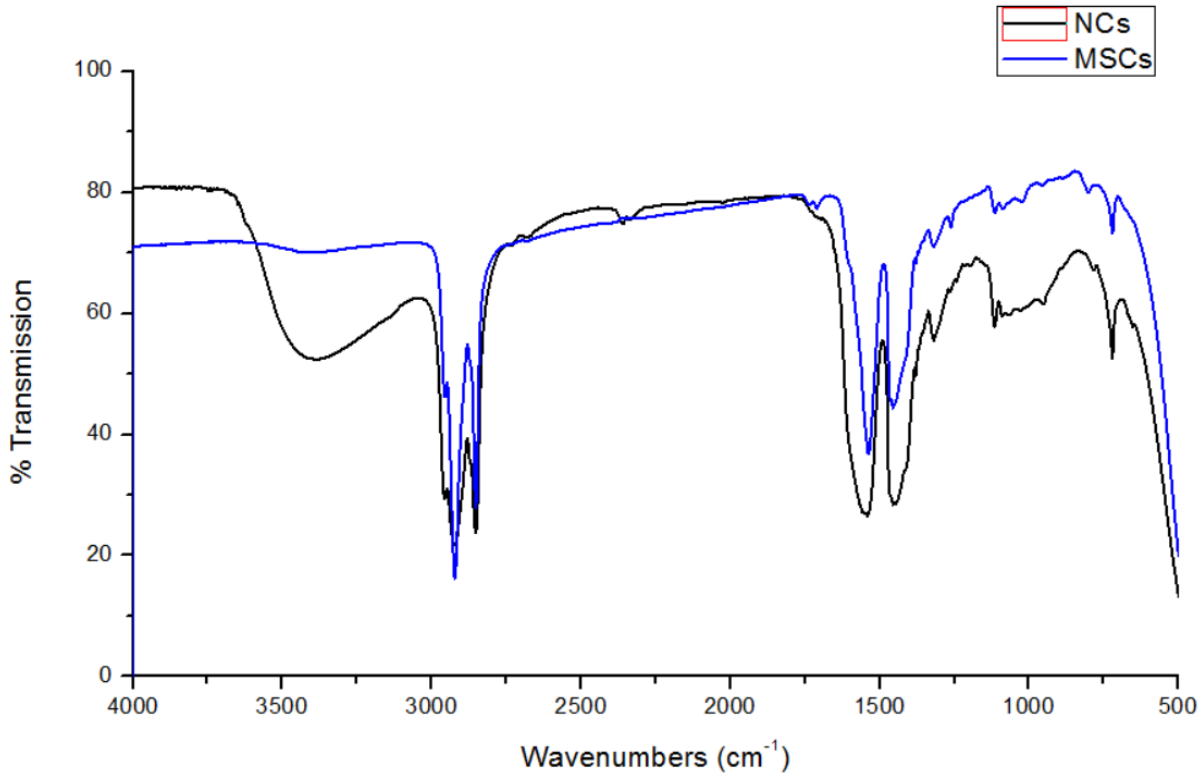

Figure 22. IR spectra comparison of clusters and purified NCs after MW reaction.

Based on the IR spectra, there is no BF_4^- coordinating to the nanocrystal surface. At 1543 & 1450 cm^{-1} are the symmetric and antisymmetric stretching of possibly free carboxylate. The peak at 1450 cm^{-1} could also correspond to C-H bending.

InP NCs synthesized with BMIm PF_6

The microwave-assisted ionic liquid synthesis was repeated using 1-butyl-3-methylimidazolium hexafluorophosphate (BMIm PF_6) as the ionic liquid to determine if it produced nanocrystals with higher QY than BMIm BF_4. The microwave reaction conditions were the same as the previous chapter. Initial microwave reactions with BMIm PF_6 IL and MSCs resulted in a sharp increase in pressure and shattering of the glass vial within the microwave

reactor. The microwave data for temperature vs. time and pressure vs. time can be seen in Figure 23. There is a huge spike in pressure which may have been due to the evolution of a gas (PF_3), possibly due to the weaker bond between phosphorous and fluorine than boron and fluorine. When comparing the magic-sized cluster precursor to separate-source precursor that our group uses, due to the cluster's purification process there is less free ligand. The lack of free, excess ligand in solution could result in less phosphorous or fluorine being trapped by the carboxylate ligands, thus possible creation of PF_3. All contents of the reaction were lost. The aftermath of the reaction can be seen in Figure 24. This reaction was done in an Anton Parr Monowave 300 and repeated in a CEM Microwave with similar results.

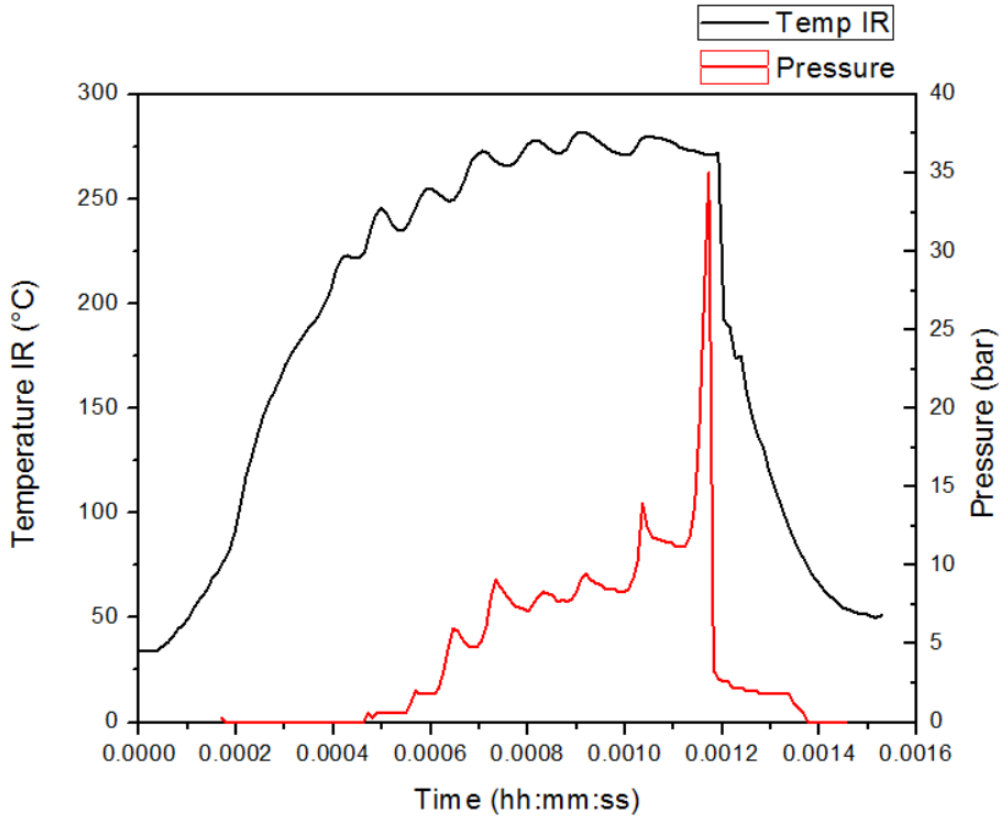

Figure 23. Temperature vs. Time and Pressure vs. Time for the Anton Paar microwave reaction with BMIm PF_6 and MSCs.

Figure 24. The microwave vial after a microwave reaction between MSCs and BMIm PF_6.

These reactions were repeated outside of the microwave on a Schlenk line in a vial under nitrogen at 230 °C and 250 °C with BMIm PF_6. Nanocrystals were produced, but the reaction conditions, such as temperature and stirring, were difficult to control. Figure 25 shows the absorbance of the nanocrystals produced at two different temperatures. We expected to see the evolution of phosphorous-fluorine species or any other boron-fluorine species because of the previous microwave reactions, but preliminary NMR studies shown in the appendix do not show any.

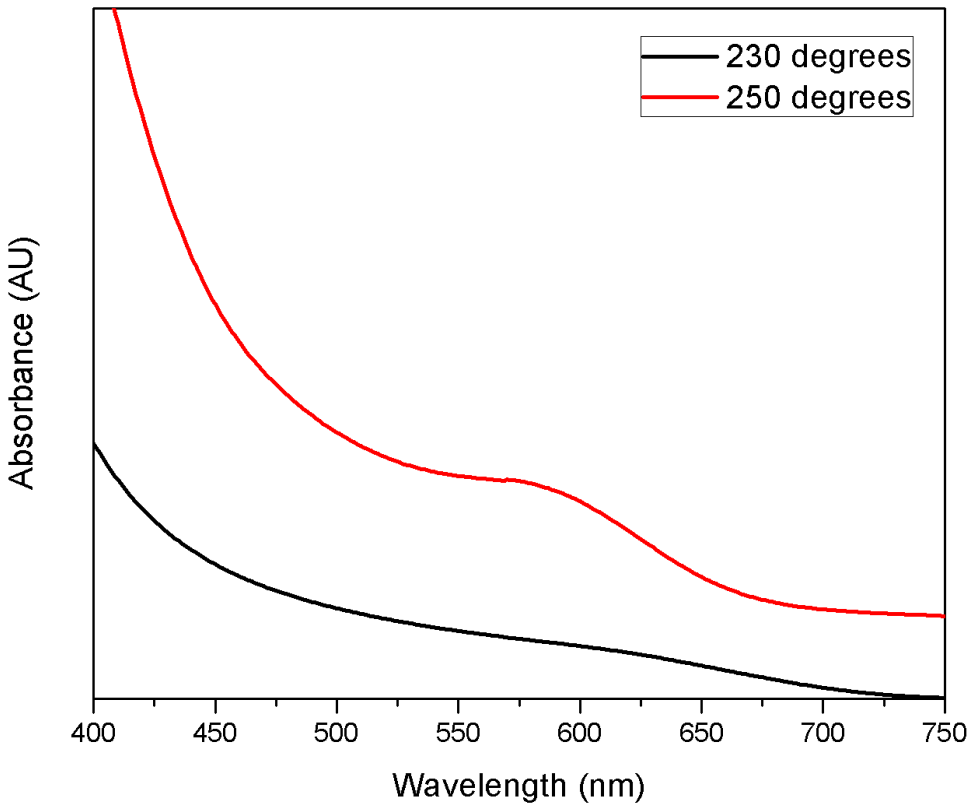

Figure 25. Absorbance of NCs produced at different temperatures with PF_6 and solid MSCs.

Ligand stripping and ligand exchange of InP NCs with BF_3:EtO_2

InP NCs that were purified with toluene and acetone then dried under vacuum were prepared for ligand stripping and exchange by resuspending them in hexanes. The BF_3:EtO_2 was prepared in DMF, then it was mixed with the InP NCs until the NCs transferred from the hexanes layer to the DMF layer.

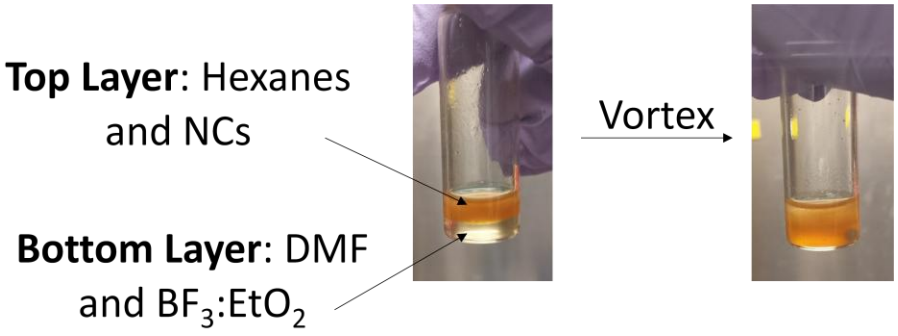

Figure 26. Nonpolar NCs transfer from hexanes in the top layer to DMF in the bottom layer and become polar.

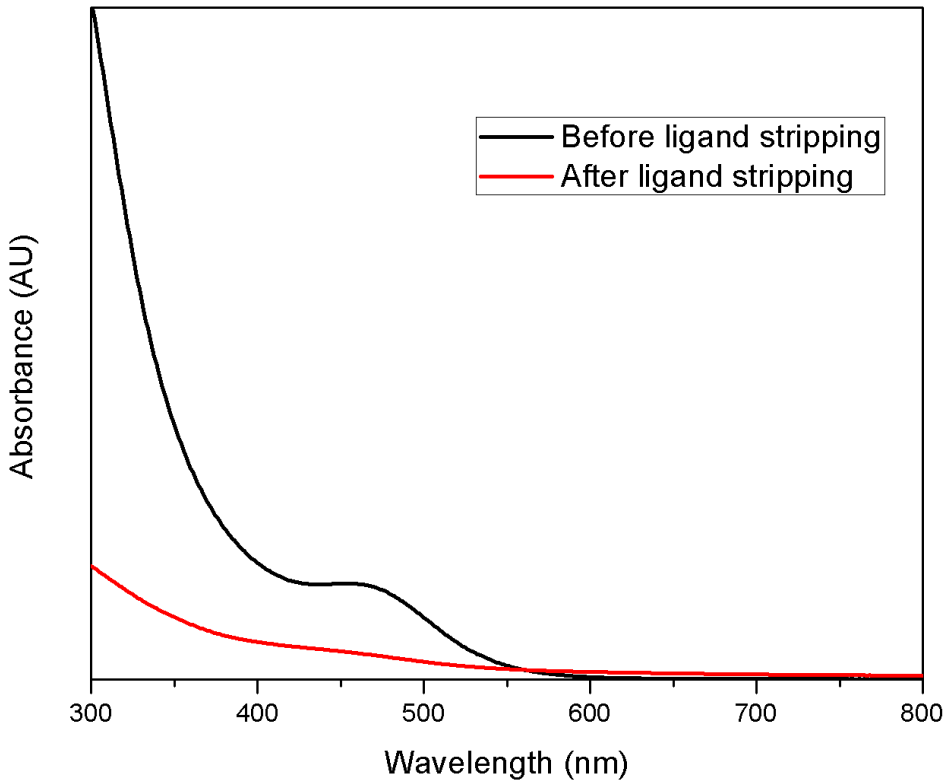

Figure 27. Absorbance spectra of nanocrystals before and after ligand stripping.

Ligand stripping or exchange does occur as the nonpolar InP NCs eventually transfer from the hexanes to DMF layer, indicating that they become polar. Sometimes after mixing, nanocrystals clumped together at the solvent interface, possibly due to incomplete removal of ligands. The polar nanocrystals were washed once with DMF and hexanes. They maintain some absorption, as seen in Figure 27, but the photoluminescence was difficult to obtain as they nanocrystals settled to the bottom of the solution. When comparing the ^{1}H NMR of the nanocrystals to myristic acid in Figure 28, there is still some myristate on the surface in addition to the solvent peaks for hexanes (0.88 and 1.26 ppm) and DMF (2.78, 2.94, and 7.96 ppm)

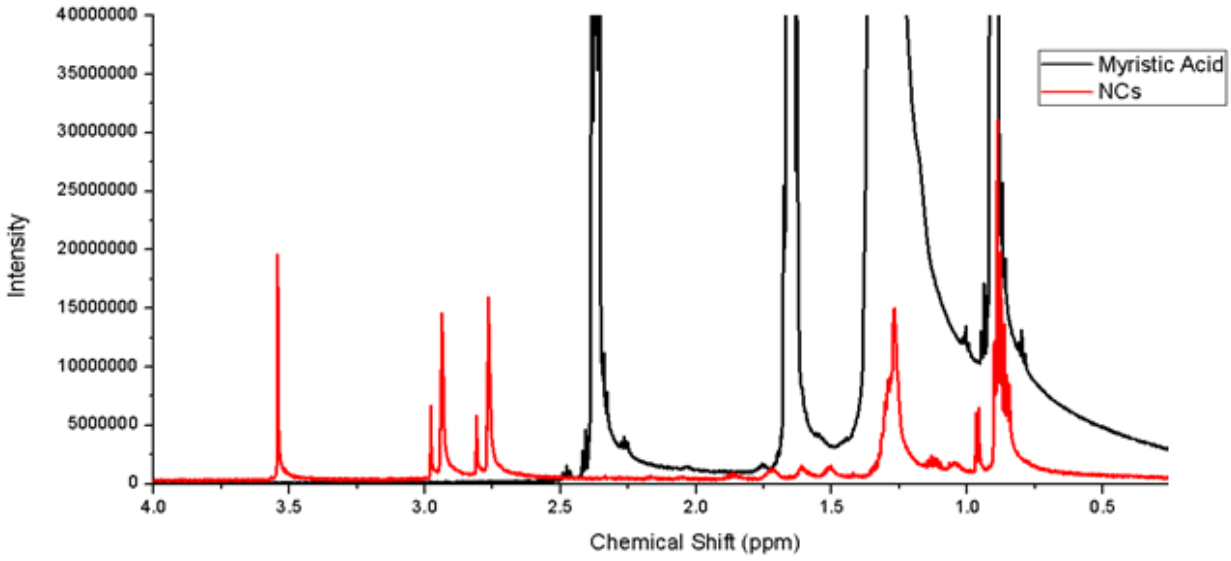

Figure 28. ^{1}H NMR comparison of polar NCs to myristic acid.

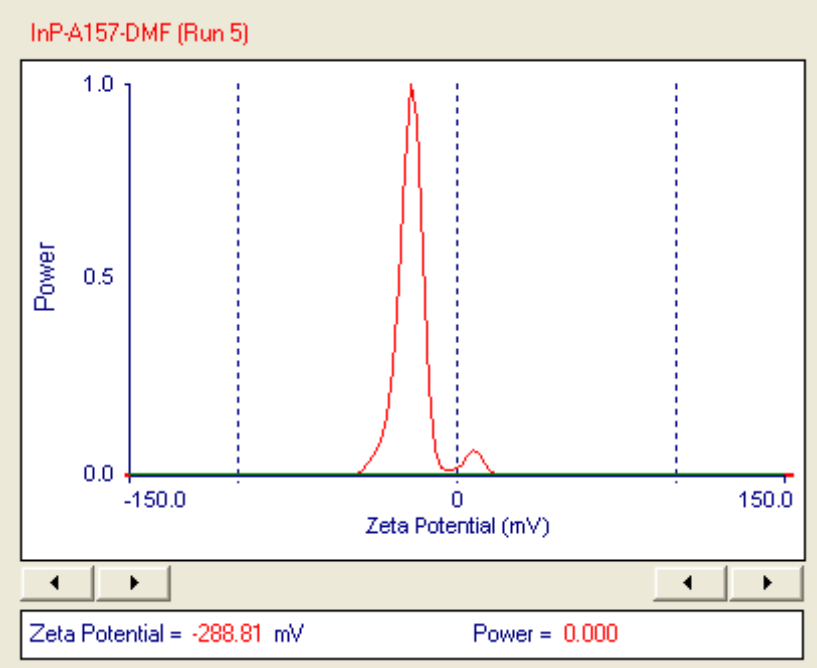

Figure 29. Zeta potential of negatively charged polar NCs.

We conducted a zeta potential measurement on the polar nanocrystals in DMF. The measurement indicates that there is possibly a very negatively charged surface, perhaps a negatively charged adduct. This, however, conflicts with the literature studies done on ligand stripped and exchanged PbSe. More studies should be done on the surface charge before making any definitive conclusions.

3.3 Conclusions

The cluster's reproducible synthesis and stability makes it a good candidate as a precursor for InP nanocrystals, as long as the temperature is strictly maintained at 110 °C and the cluster stored as a solid under inert atmosphere. Absorbance and photoluminescence spectra confirm that we can produce luminescent InP NCs using the cluster as our precursor instead of previously

used solution-based, red separate-source precursor. Based on the FWHM, the quality of the NCs made with MSCs is comparable to NCs made with the separate source precursor. When examining the nanocrystal surface, there are still free myristate ligands in solution. From the NMR, there may still be TMS that had not been fully purified from the clusters. There are not, however, any boron-fluorine compounds on the nanocrystal surface, which is due to BF_4^- stability. There is no evidence of any phosphorous-fluorine species, which would have indicated that fluoride is binding to phosphorous species on the surface. No peaks observed in ^{19}F NMR for InP NCs, because the boron-fluorine bond in BF_4^- is very stable, so it will not readily decompose and release fluoride ions. There may be BF_4^- carboxylate adducts as BF_3 is a good Lewis acid and will form adducts with Lewis bases, but we do not observe any. More studies should be done to examine how fluorine species are reacting with the nanocrystal surface. When attempting to produce nanocrystals with BMIm PF_6, a gas in the microwave was produced on 2 separate occasions. Based on microwave data, an increase in pressure was observed. When repeating the reactions in a vial on a Schlenk line, nanocrystals were produced.

InP nanocrystals maintain a slightly diminished luminescence in polar solvent after ligand stripping. Initial Zeta-potential data reports that the nanocrystals have a negatively charged surface, despite literature reports for positively charged PbSe. This means that there are negatively charged anions, possibly an adduct of $[BF_n(O_2CR)_{4-n}]^-$ species as BF_3 is a good Lewis acid it forms an adduct with carboxylate, or DMF, on a positively charged, indium rich core. More studies, such as further Zeta-potential measurements and NMR, should be conducted into the surface of the ligand stripped InP.

3.4 Experimental

Synthesis of Indium Myristate (InMA)

An air condenser, rubber septum, and temperature controller were attached to a 100 mL three-neck round bottom flask. The schlenk line was degassed until it reached baseline pressure. Indium acetate (0.465 g, 3.2 mmol) and myristic acid (1.325 g, 11.6 mmol) were added to the round bottom flask and evacuated for 20 min until pressure reached baseline. The solids were then heated to 100 °C under vacuum for approximately 6 hours to remove any acetic acid produced. A heat gun was used to melt any reactants on the sides of the flask. Taken from the glovebox, 10 mL of dry toluene was added to the flask. The reaction was heated overnight under nitrogen for approximately 12 hours.

Synthesis of Magic-Sized Clusters (MSCs)

In an argon filled glovebox, 1.15 mL (0.55 mmol) of tris(trimethylsilyl)phosphine ($P(TMS)_3$) in 5 mL toluene was drawn into a syringe and sealed with a rubber stopper. After heating the $In(MA)_3$ to 110 °C, the $P(TMS)_3$ mixture was injected into the flask. Cluster growth was monitored by taking aliquots, adding the aliquot to hexanes, and measuring their absorption. Clusters were grown for approximately 40 minutes until they reached an absorbance of 386 nm.

MSCs Workup Procedure

After reaching the desired size, the reaction was quenched by removing from heat. The toluene was evaporated from the flask until dry, then the flask was brought into an argon filled glove box. The clusters were resuspended in 5 mL of toluene. then 2 more mL of toluene was used to rinse the flask. The clusters were centrifuged to separate excess ligands. The resulting

supernatant was transferred to new centrifuge tubes, and the solids were confirmed by NMR as myristic acid. The clusters in the supernatant was precipitated with acetonitrile and centrifuged. The resulting supernatant was discarded. The MSCs were resuspended in a minimal amount of toluene, precipitated with acetonitrile, and centrifuged. This procedure was repeated three more times. Finally, the clusters were resuspended in pentane and the flask was evacuated to remove any remaining solvent. The clusters were stored as a solid in the glovebox.

Microwave-Assisted InP NC Synthesis

Samples were prepared in a glovebox under inert atmosphere using capped 10 mL Pyrex glass microwave vessels with a stir bar. MSC precursor (3 mL) and the ionic liquid, 1-methyl-3-butylimidazoliumtetrafluoroborate was added to a microwave vessel and capped. The same microwave parameters and purification procedure as the previous section were used.

Synthesis of InP NCs with BMIm PF_6

Some waxy, solid, solvent free clusters was added to 100 μL of IL. (Clusters were difficult to weigh because they were waxy). The clusters and IL were heated in vial for 10 minutes in oil bath under nitrogen. Reactions were conducted at approximately 230 °C and 252 °C to closely mimic the set microwave temperature as much as possible.

Ligand stripping and ligand exchange of InP NCs with BF_3:EtO_2

This procedure was adapted from Helms *et al*. NCs that were synthesized using MSCs and BMIM BF_4 ionic liquid were dissolved in 500 uL of hexanes. 20 uL of BF_3:$Et0_2$ was dissolved in 500 uL of DMF. This solution was then added to the NCs, and the solution was

agitated until the NCs transferred from the hexanes layer to the DMF layer. The nanocrystals were washed in DMF and centrifuged.

The UV-Vis absorbance spectra were obtained using a Cary 5000 UV-Vis-NIR Spectrophotometer. The NMR spectra were obtained in deuterated $CDCl_3$ using Varian 400 MHz or Bruker WB 600 MHz NMR spectrometers. The IR spectra were obtained using a Nicolet FT-IR Spectrometer.

References

(1) Grim, J. Q.; Manna, L.; Moreels, I. A Sustainable Future for Photonic Colloidal Nanocrystals. *Chem. Soc. Rev.* **2015**, *44* (16), 5897–5914.

(2) Kumar, P.; Singh, S.; Gupta, B. K. Future Prospects of Luminescent Nanomaterial Based Security Inks: From Synthesis to Anti-Counterfeiting Applications. *Nanoscale* **2016**, *8* (30), 14297–14340.

(3) Gary, D. C.; Terban, M. W.; Billinge, S. J. L.; Cossairt, B. M. Two-Step Nucleation and Growth of InP Quantum Dots via Magic-Sized Cluster Intermediates. *Chem. Mater.* **2015**, *27* (4), 1432–1441.

(4) Gary, D. C.; Flowers, S. E.; Kaminsky, W.; Petrone, A.; Li, X.; Cossairt, B. M. Single-Crystal and Electronic Structure of a 1.3 Nm Indium Phosphide Nanocluster. *J. Am. Chem. Soc.* **2016**, *138* (5), 1510–1513.

(5) Carey, G. H.; Abdelhady, A. L.; Ning, Z.; Thon, S. M.; Bakr, O. M.; Sargent, E. H. Colloidal Quantum Dot Solar Cells. *Chem. Rev.* **2015**, *115* (23), 12732–12763.

(6) Tang, J.; Kemp, K. W.; Hoogland, S.; Jeong, K. S.; Liu, H.; Levina, L.; Furukawa, M.; Wang, X.; Debnath, R.; Cha, D.; et al. Colloidal-Quantum-Dot Photovoltaics Using Atomic-Ligand Passivation. *Nat. Mater.* **2011**, *10* (10), 765–771.

(7) Park, J. P.; Lee, J.-J.; Kim, S.-W. Highly Luminescent InP/GaP/ZnS QDs Emitting in the Entire Color Range via a Heating up Process. *Sci. Rep.* **2016**, *6*.

(8) Kim, S.; Kim, T.; Kang, M.; Kwak, S. K.; Yoo, T. W.; Park, L. S.; Yang, I.; Hwang, S.; Lee, J. E.; Kim, S. K.; et al. Highly Luminescent InP/GaP/ZnS Nanocrystals and Their Application to White Light-Emitting Diodes. *J. Am. Chem. Soc.* **2012**, *134* (8), 3804–3809.

(9) Talapin, D. V.; Gaponik, N.; Borchert, H.; Rogach, A. L.; Haase, M.; Weller, H. Etching of Colloidal InP Nanocrystals with Fluorides: Photochemical Nature of the Process Resulting in High Photoluminescence Efficiency. *J. Phys. Chem. B* **2002**, *106* (49), 12659–12663.

(10) Adam, S.; Talapin, D. V.; Borchert, H.; Lobo, A.; McGinley, C.; de Castro, A. R. B.; Haase, M.; Weller, H.; Möller, T. The Effect of Nanocrystal Surface Structure on the Luminescence Properties: Photoemission Study of HF-Etched InP Nanocrystals. *J. Chem. Phys.* **2005**, *123* (8), 084706.

(11) Lovingood, D. D.; Strouse, G. F. Microwave Induced In-Situ Active Ion Etching of Growing InP Nanocrystals. *Nano. Lett.* **2008**, *8* (10), 3394–3397.

(12) Siramdas, R.; McLaurin, E. J. InP Nanocrystals with Color-Tunable Luminescence by Microwave-Assisted Ionic-Liquid Etching. *Chem. Mater.* **2017**, *29* (5), 2101–2109.

(13) Doris, S. E.; Lynch, J. J.; Li, C.; Wills, A. W.; Urban, J. J.; Helms, B. A. Mechanistic Insight into the Formation of Cationic Naked Nanocrystals Generated under Equilibrium Control. *J. Am. Chem. Soc.* **2014**, *136* (44), 15702–15710.

(14) Talapin, D. The surface science of nanocrystals. *Nat. Mater.* **2016**, *15*, 141–153.

(15) Ning, J.; Banin, U. Magic Size InP and InAs Clusters: Synthesis, Characterization and Shell Growth. *Chem. Commun.* **2017**, *53* (17), 2626–2629.

(16) Allen, P. M.; Walker, B. J.; Bawendi, M. G. Mechanistic Insights into the Formation of InP Quantum Dots. *Angew. Chem.* **2010**, *49* (4), 760–762.

(17) Ritchhart, A.; Cossairt, B. Templated Growth of InP Nanocrystals with a Polytwistane Structure. *Angew. Chem.* n/a-n/a.

Chapter 4 - Conclusions

InP nanocrystals were predominantly modified using post-synthetic methods such as shell growth, which is a time consuming process, or dangerous acids like HF. In this thesis, we demonstrate that single-source precursors like the InP magic-sized cluster are reproducible, more stable over time, and capable of producing luminescent nanocrystals in a microwave reactor without the need for post-synthetic modification.

The microwave-assisted ionic liquid synthesis rivals previous syntheses as it is shorter, requires less material, and safer. The 1:10 ratio of separate-source precursor to the BMIm BF_4 ionic liquid can achieve quantum yields up to 21%, but there are factors, such as how the microwave interacts with larger quantities of ionic liquid (results in arcing), precursor longevity, and when the reactions are conducted (consecutively or not), that can affect the absorption and PL of the nanocrystals. When BMIm PF_6 is used as the ionic liquid, gas is produced, thus creating a hazardous, high pressure microwave reaction. This reaction can produce nanocrystals when performed on a Schlenk line.

When beginning to examine how ionic liquids passivate the nanocrystal surface, based on ^1H NMR and IR, there are no boron-fluorine or phosphorous-fluorine species on the nanocrystal surface. This is likely due to the stability of BF_4. $[BF_n(O_2CR)_{4-n}]^-$ species could be produced from reactions with BF_4 and native carboxylate surface ligands. There is the appearance of a BF_3 peak, possibly an adduct with carboxylate, but more studies should be done to corroborate this.

In the future, focusing on understanding the mechanistic relationship between ionic liquids and InP precursors can lead to more efficient syntheses for highly luminescent InP nanocrystals.

Appendix A - InP Nanocrystals

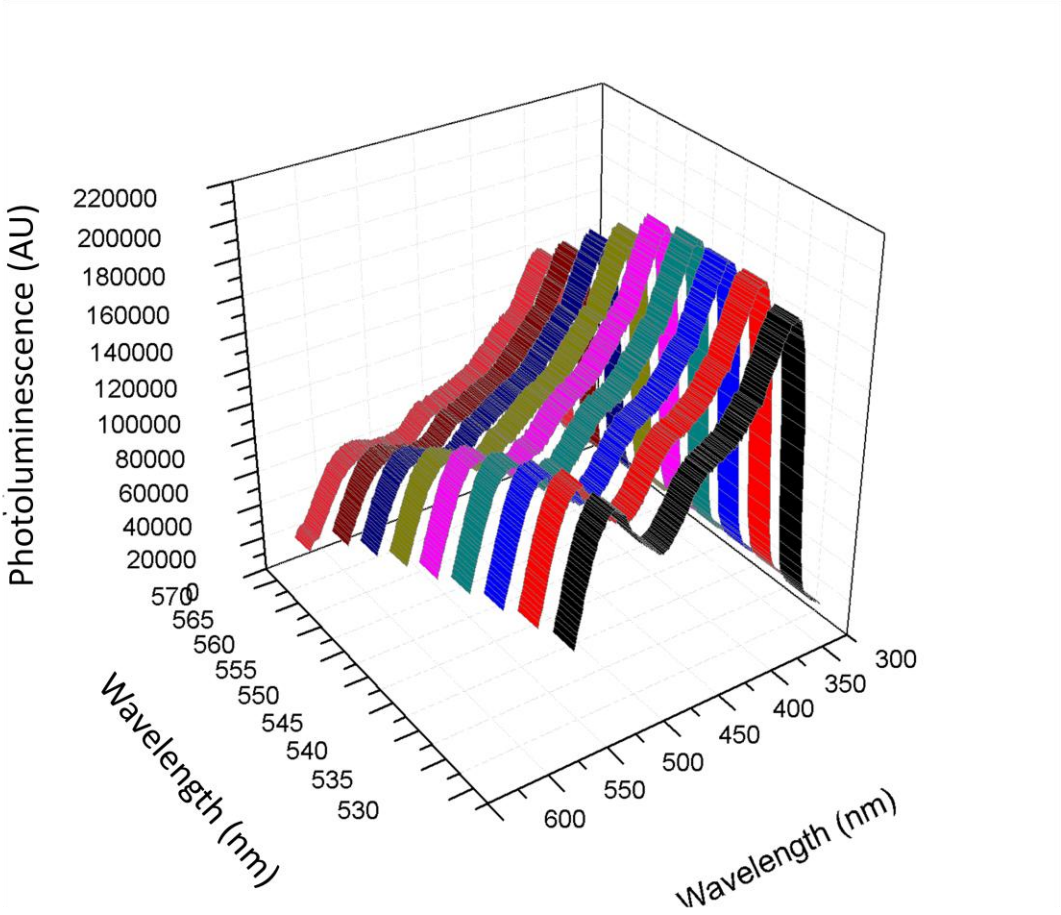

Figure 30. 3D photoluminescence excitation plot of InP NCs at different excitation wavelengths to look at sample homogeneity.. The scans were taken of the supernatant of a sample prepared with 1:10 ratio of separate-source precursor to BMIm BF_4.

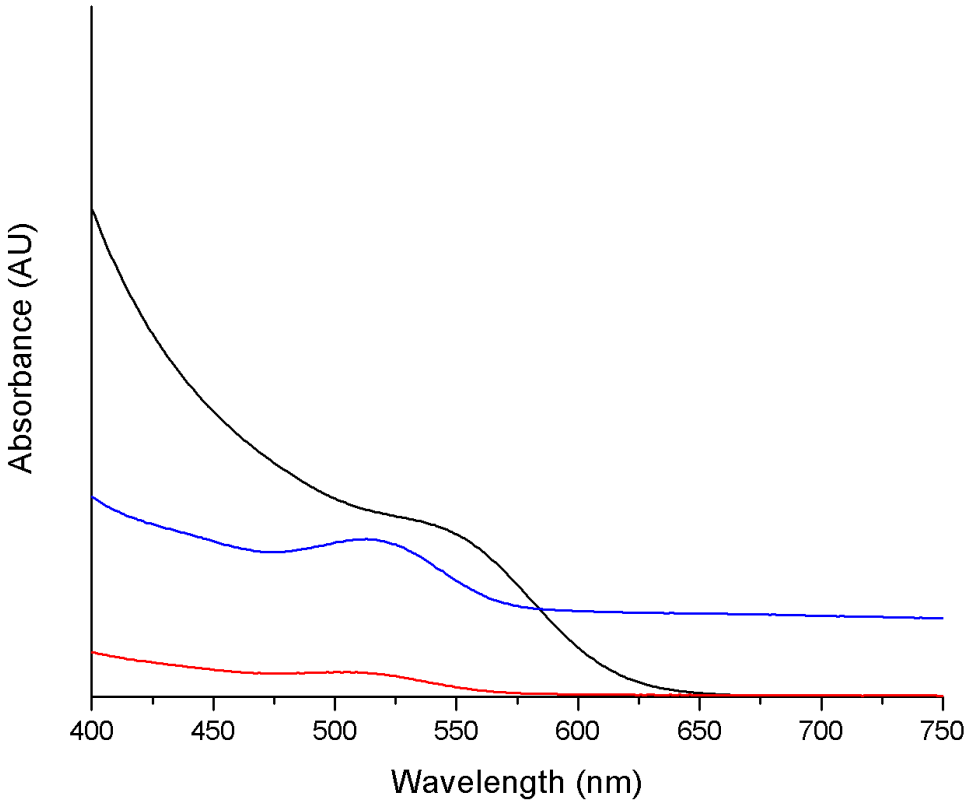

Figure 31. Absorption plot of three separate experiments for 1:1 ratio of separate-source precursor to BMIm BF_4.

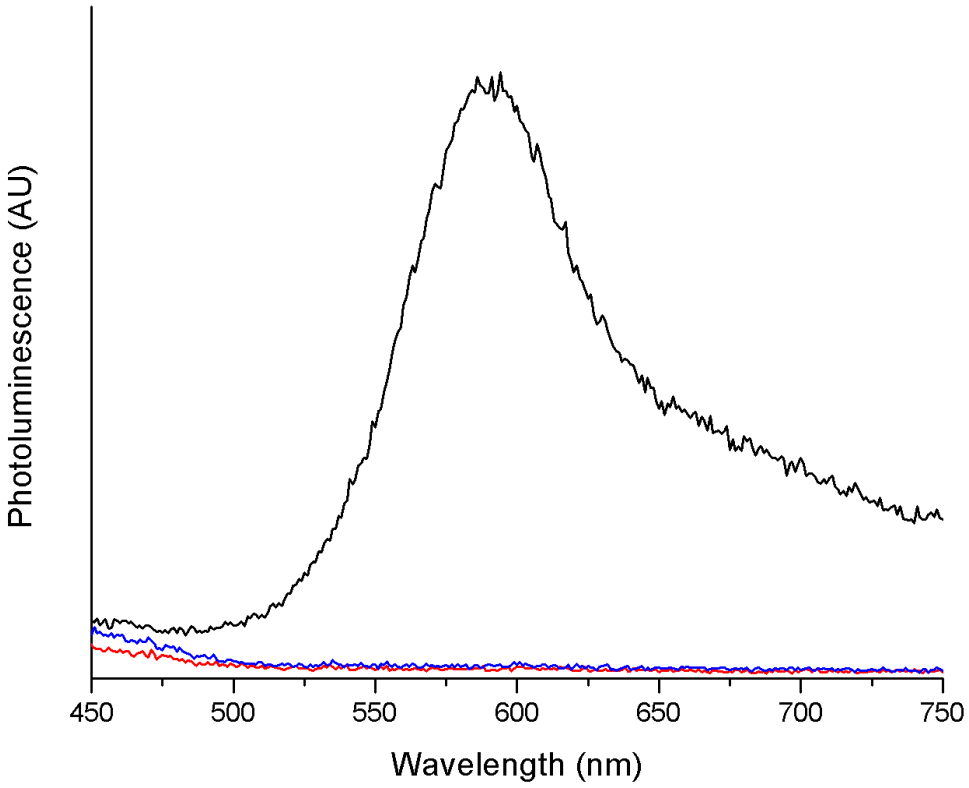

Figure 32. PL plot of three separate experiments for 1:1 ratio of separate-source precursor to BMIm BF_4.

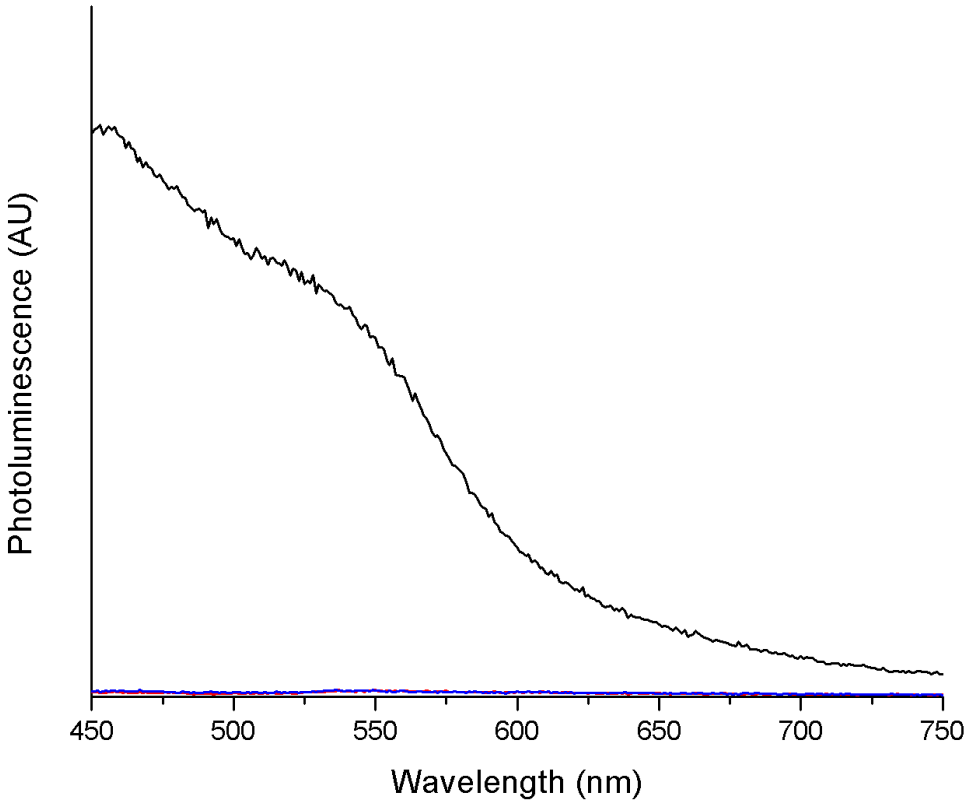

Figure 33. PL spectra of supernatant from 1st purification step for two separate experiments for 1:1 ratio of separate-source precursor to BMIm BF_4.

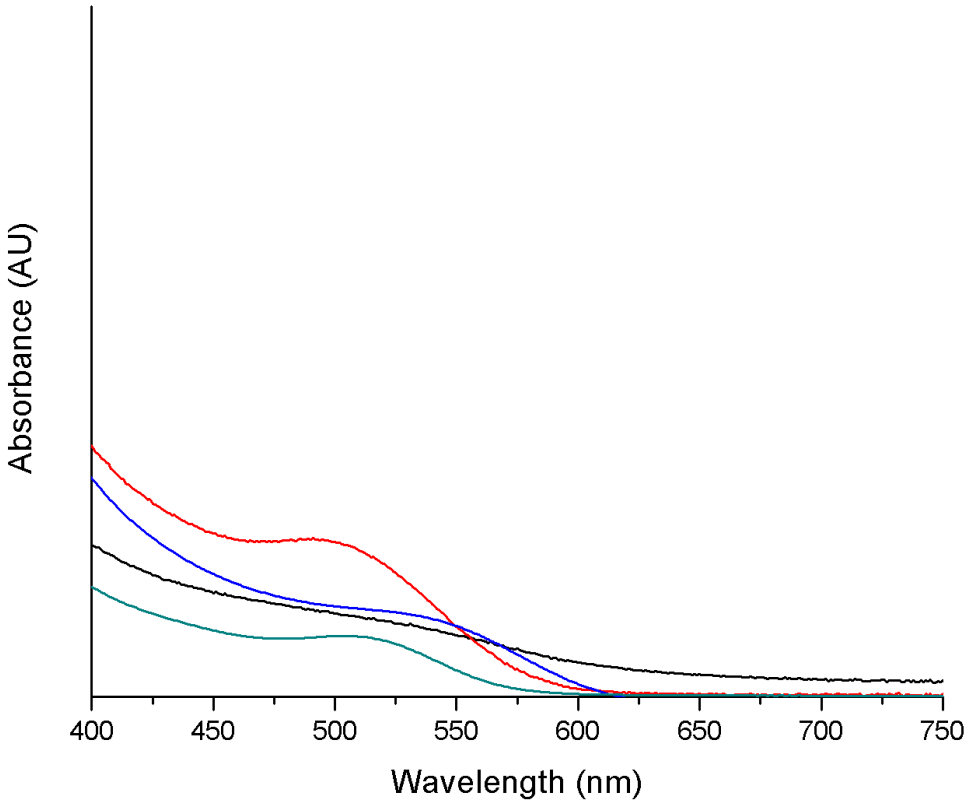

Figure 34. Absorption spectra of three separate experiments for 1:10 ratio of separate-source precursor to BMIm BF_4.

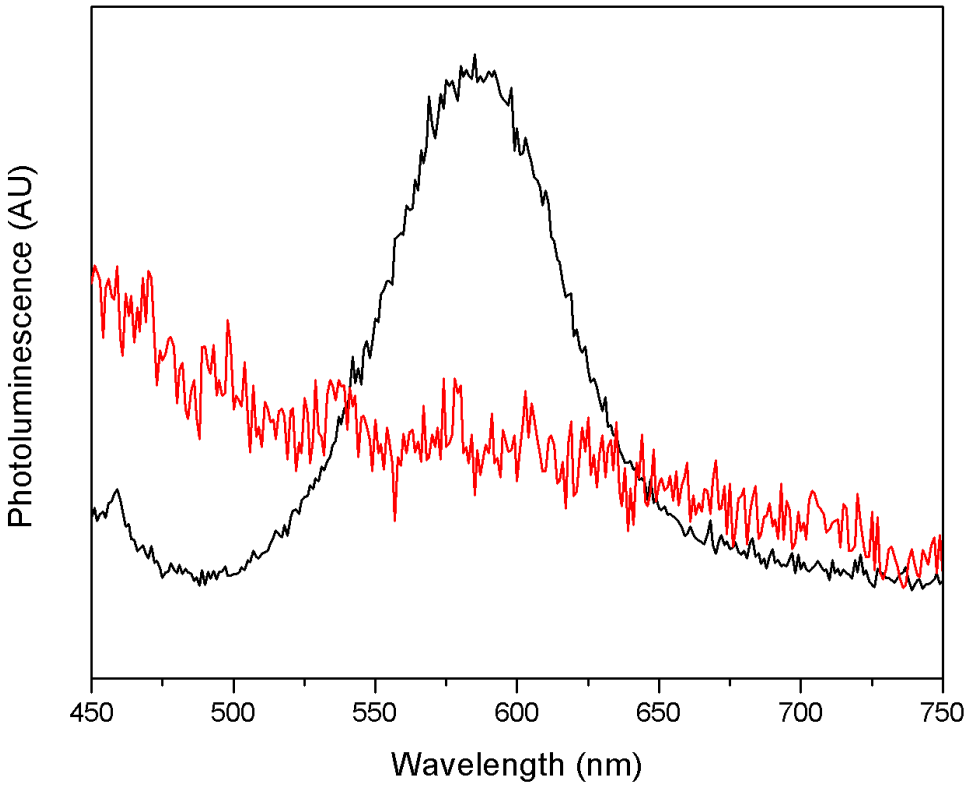

Figure 35. PL spectra of two separate experiments for 1:10 ratio of separate-source precursor to BMIm BF_4.

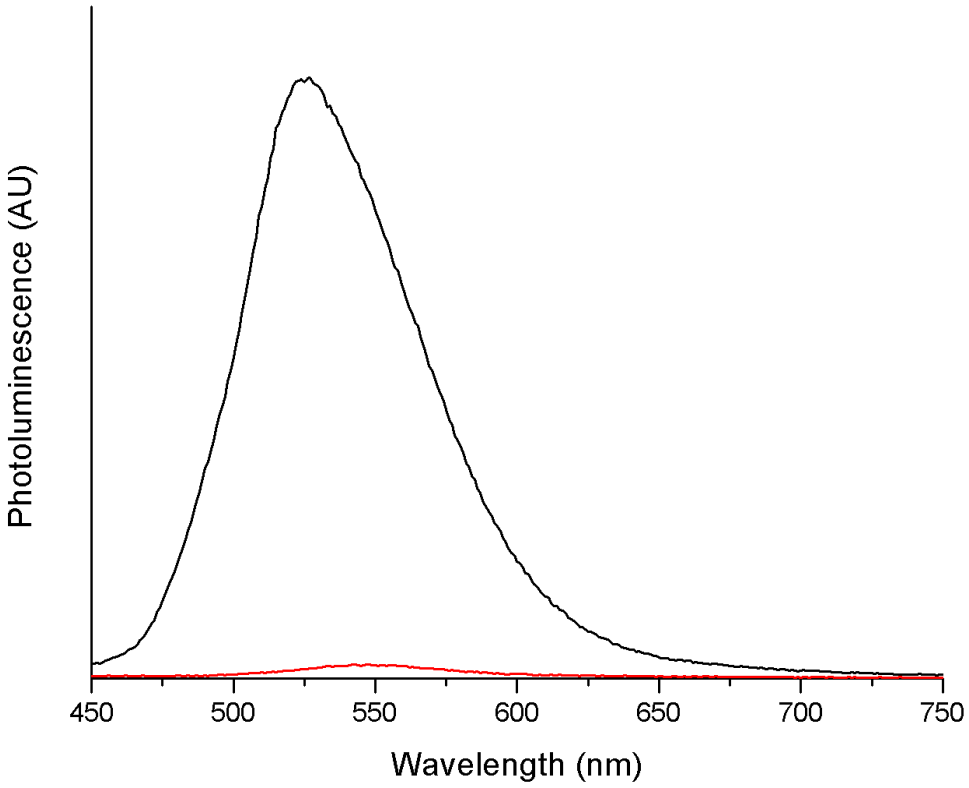

Figure 36. PL spectra of two separate experiments for 1:10 supernatant ratio of separate-source precursor to BMIm BF_4.

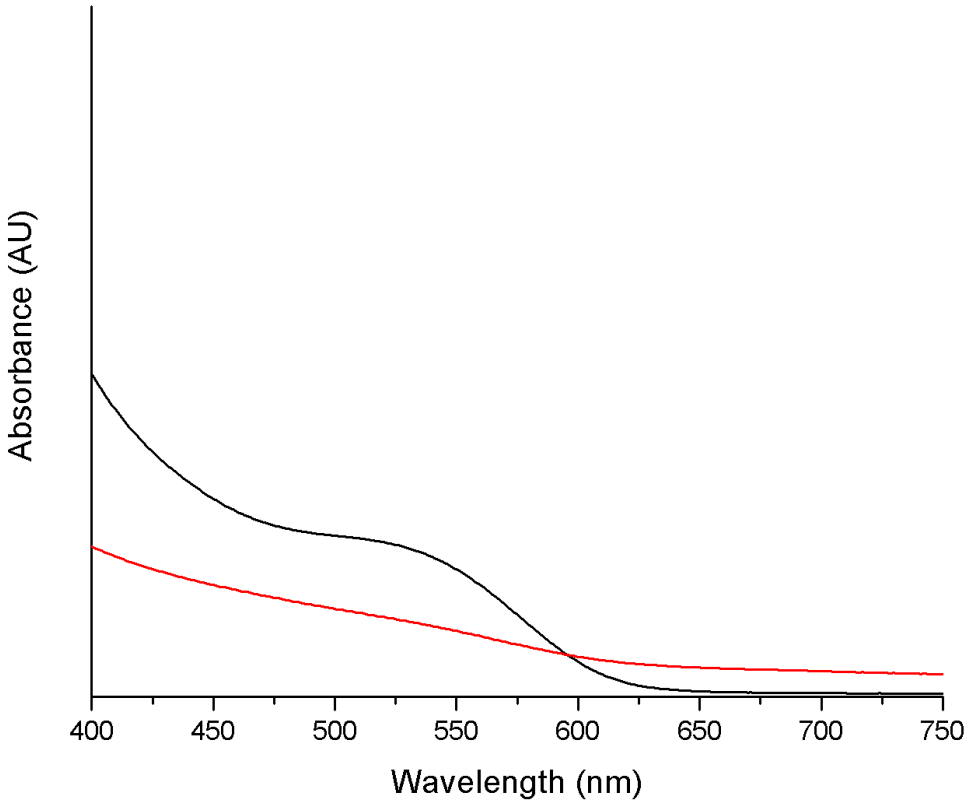

Figure 37. Absorption spectra of two separate experiments for 1:50 ratio of separate-source precursor to BMIm BF_4.

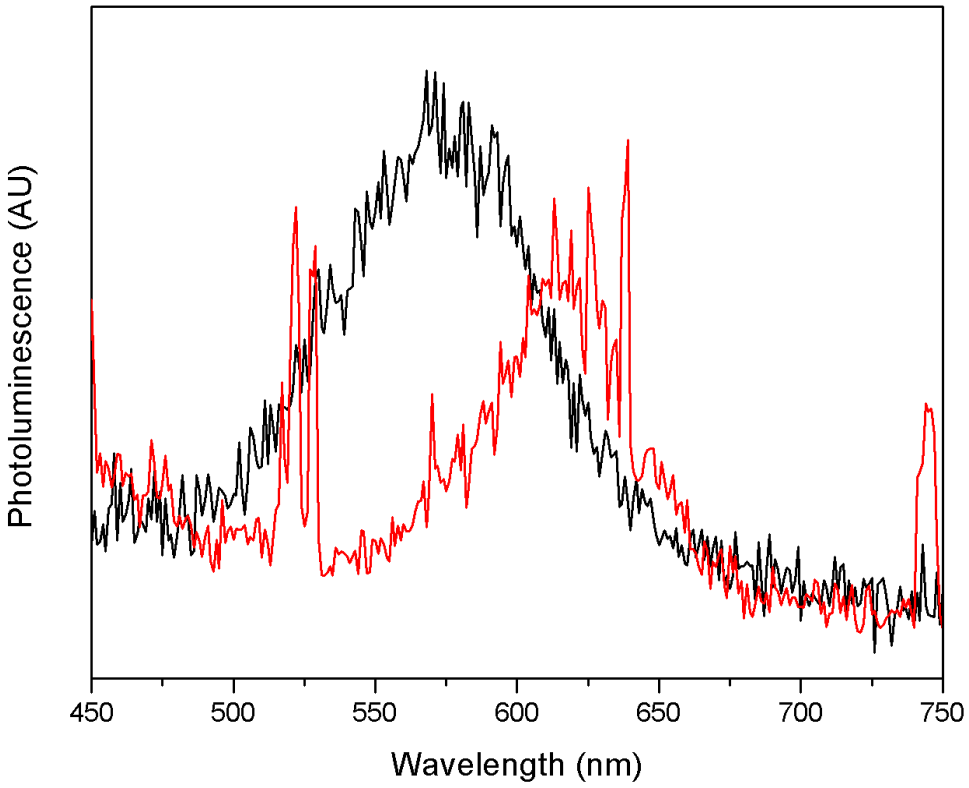

Figure 38. PL spectra of two separate experiments for 1:50 ratio of separate-source precursor to BMIm BF_4.

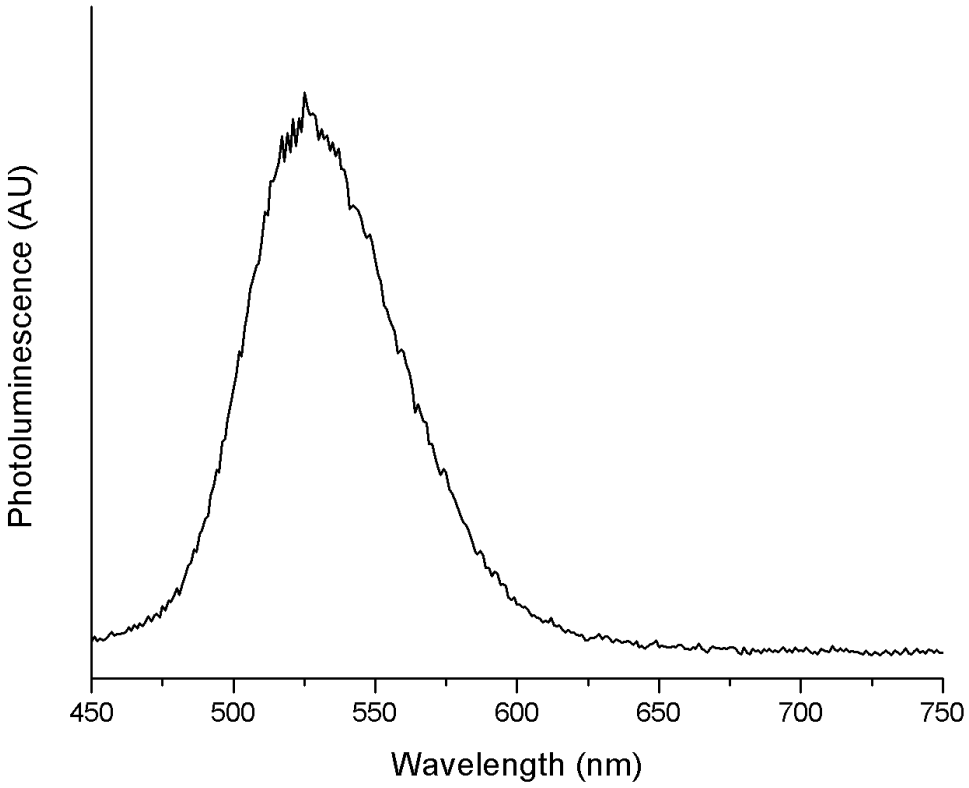

Figure 39. PL spectrum for the supernatant of the 1:50 ratio of separate-source precursor to BMIm BF_4.

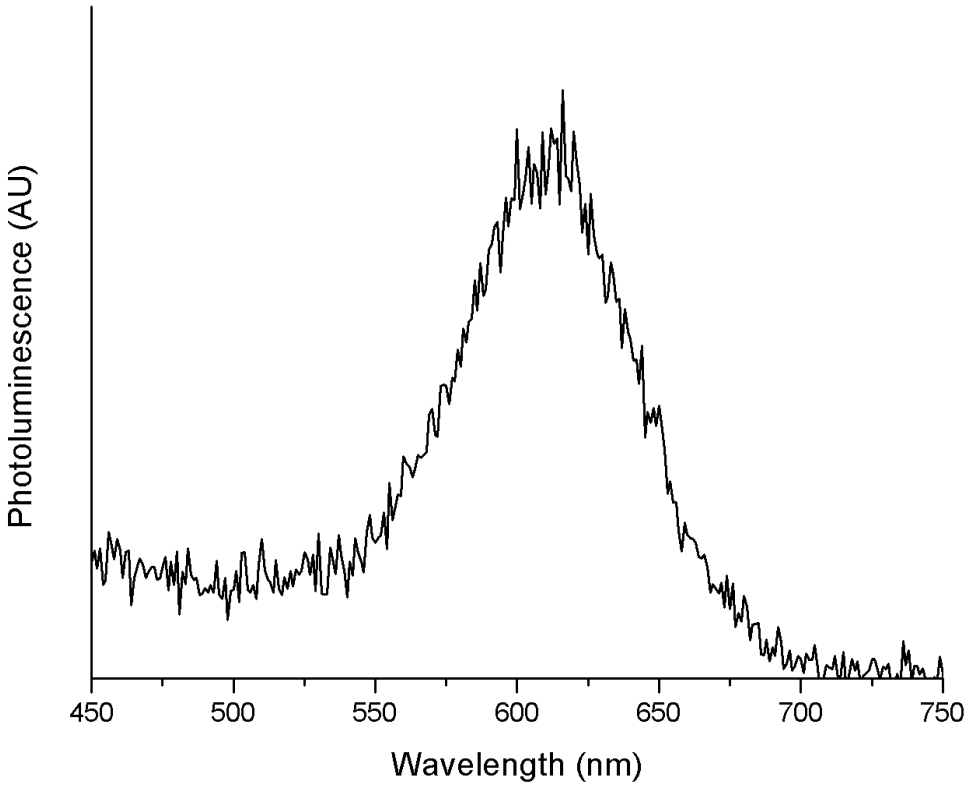

Figure 40. PL spectrum for supernatant 1:75 ratio of separate-source precursor to BMIm BF_4.

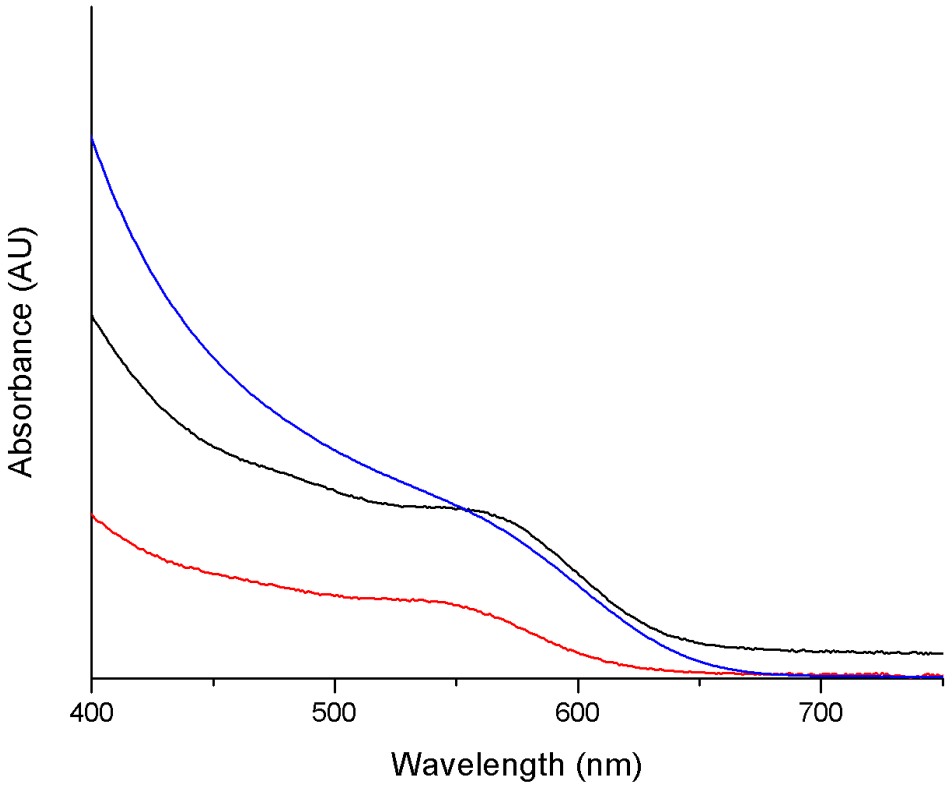

Figure 41. Absorption spectra of three separate experiments for 1:100 ratio of separate-source precursor to BMIm BF_4.

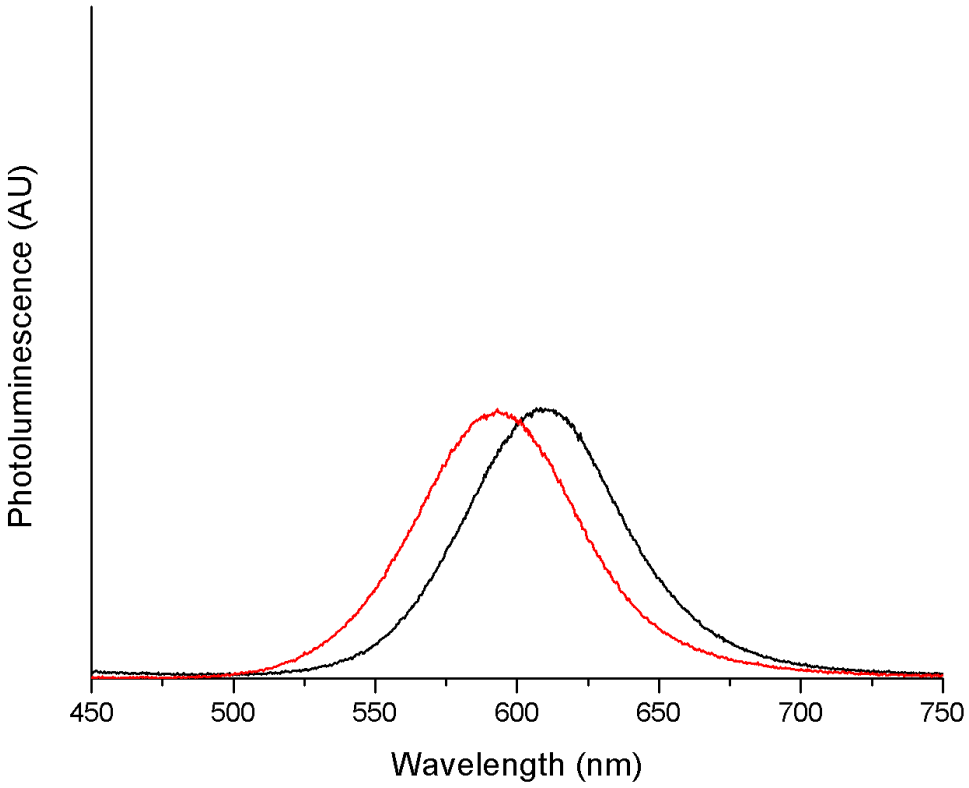

Figure 42. PL spectra of two separate experiments for for 1:100 ratio of separate-source precursor to BMIm BF_4.

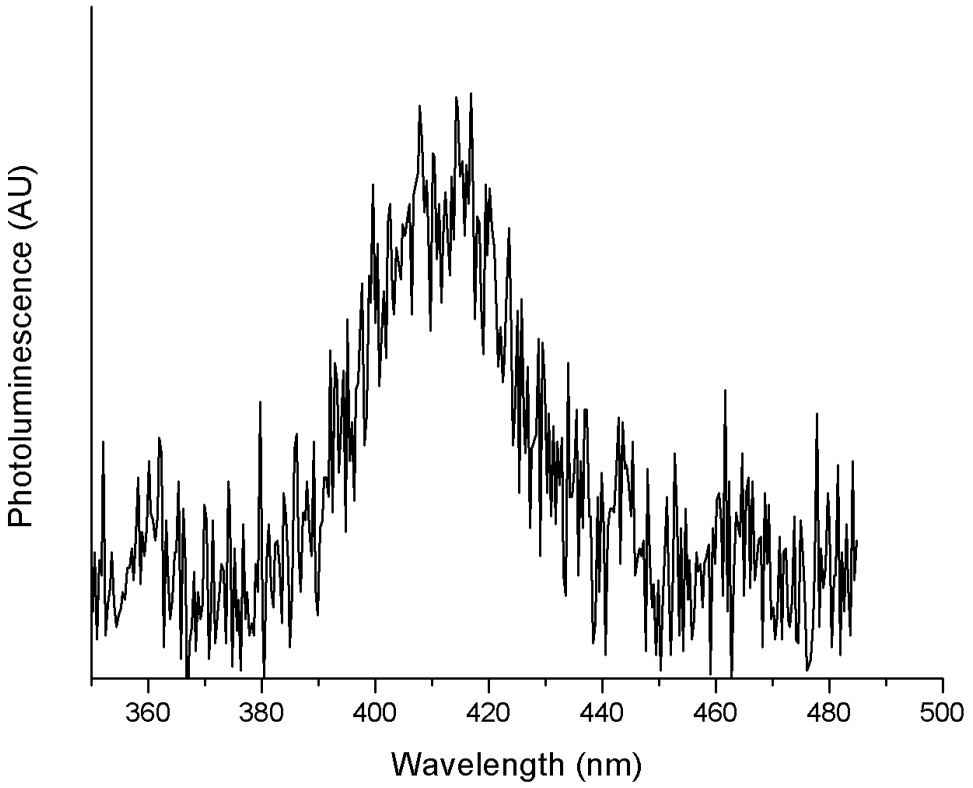

Figure 43. PL spectrum for another 1:100 ratio of separate-source precursor to BMIm BF_4.

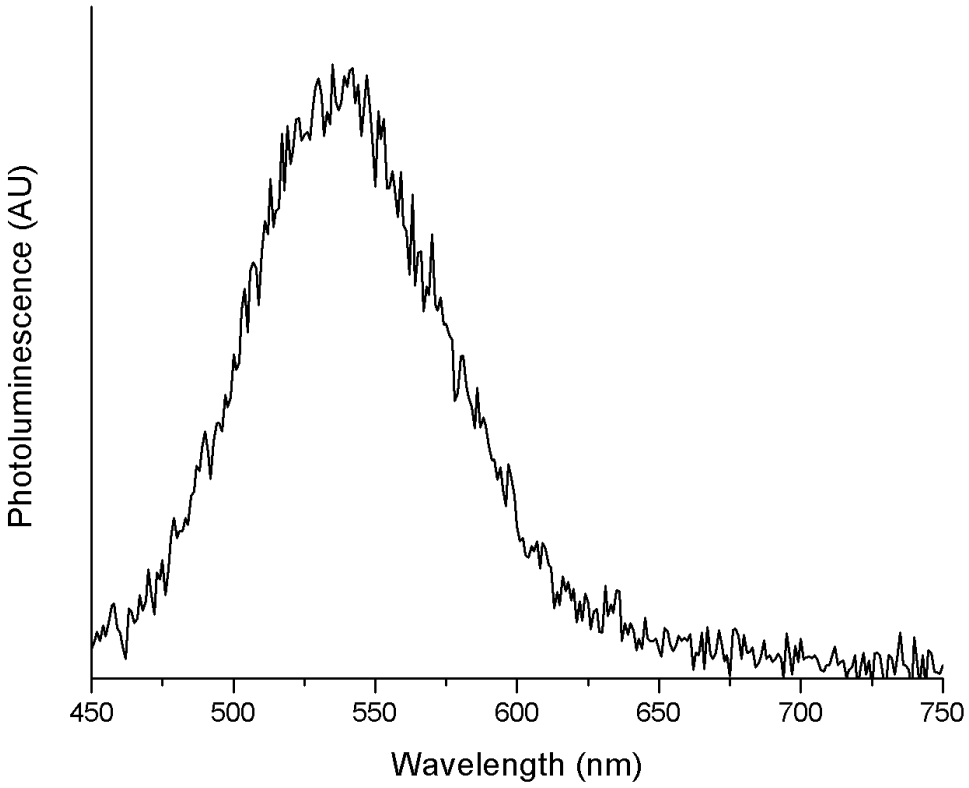

Figure 44. PL spectrum for supernatant 1:100 ratio of separate-source precursor to BMIm BF_4.

Ratio	Dye	QY (%)
1:1	Fluorescein	1.6

	Fluorescein	<0.1
1:1 supernatant	Rhodamine B Rhodamine B	3.2 3.1
1:10	Fluorescein Fluorescein	0.4 <0.1
1:10 supernatant	Fluorescein Fluorescein	1.1 21
1:50	Rhodamine B Rhodamine B	5.3 4.4
1:50 supernatant	Rhodamine B	18.8
1:75	Rhodamine B	<0

Table 2. Quantum yield measurements for each ratio's experiment conducted. Each experiment that was repeated is shown in the table to highlight the variation in experiments.

As the volume of ionic liquids increases, the power settings of the microwave reactor had to be adjusted. Higher volumes of ionic liquid caused more interactions with the pulsing magnetic field, which results in arcing. Ionic compounds will generate their own electric field in the presence of microwaves. When there is a higher volume of ionic liquid, a larger electric field was likely generated and possibly not dissipated in the form of heat very quickly, so sparks are given off. The microwave reactor discontinued the reaction as a safety precaution. For 1:100, less power was used (300 W) to decrease the likelihood of inducing sparks.

Appendix B - MSCs with BMIm PF_6

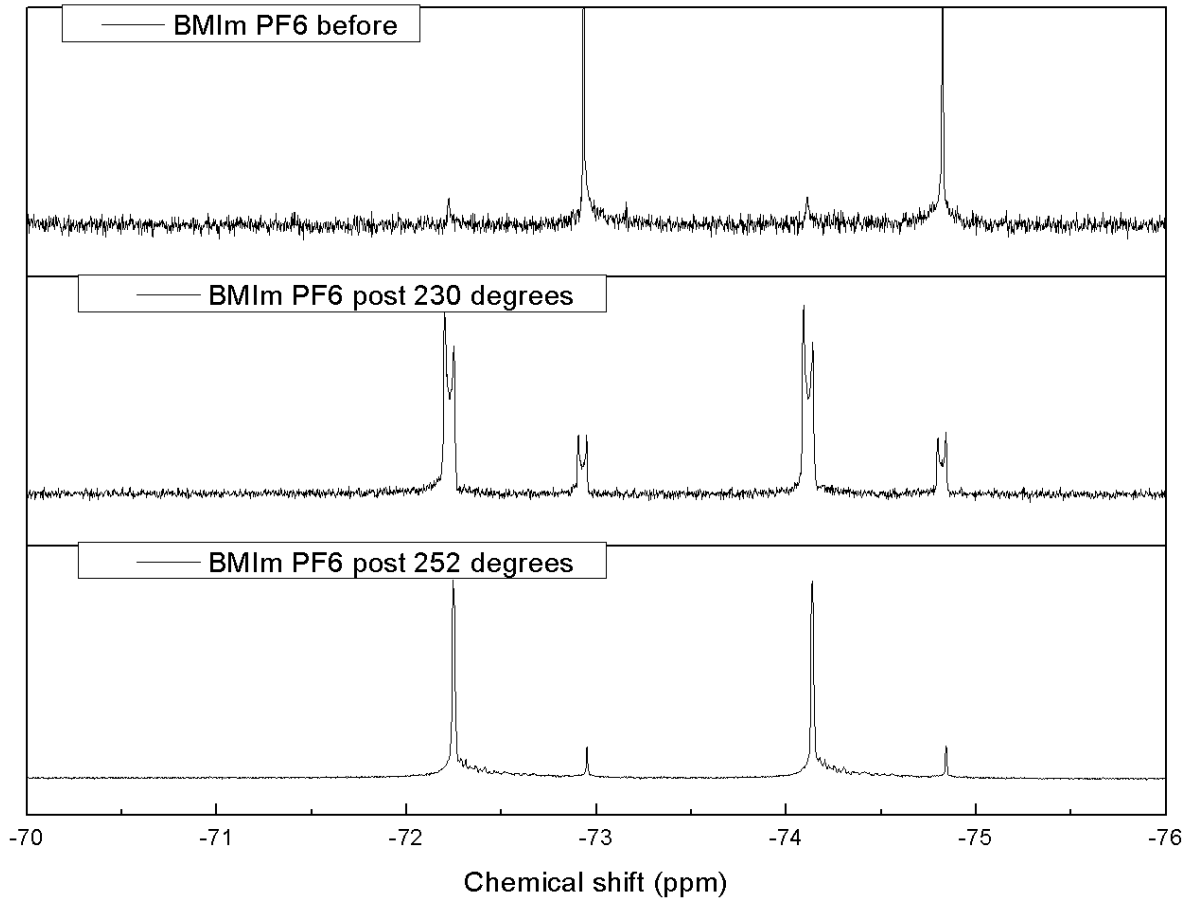

Figure 45. ^{1}H NMR of BMIm PF_6 before and after nanocrystal synthesis on a Schlenk line at 230 °C and 252 °C.

Appendix C - Control Experiments

We ran control experiments to verify side-product formation on the nanocrystals surfaces that could affect the QD properties. Determined if the control experiments would react at room temperature and form side products such as $[B(O_2C)_xF_{4-x}]$ and $Me_xSiF_{4-x.}$

OA reactions

A OA:BF_3 adduct peak (5.2-5.0 ppm) was expected to appear in the NMR spectrum. Only the alkene peak appeared around 5.35 ppm, no adduct found.

$In(OAc)_3$ reaction

$In(OAc)_3$ was insoluble in solvents used so there was barely any reaction. Unknown peaks are thought to be related to oxygen bonding, further analysis is required.

Phosphine reactions

Every reaction changed color. Series of unknown peaks could be $P(NMe_2)_3$:BF_3 adducts or phosphorous dimers that may cause the color change.

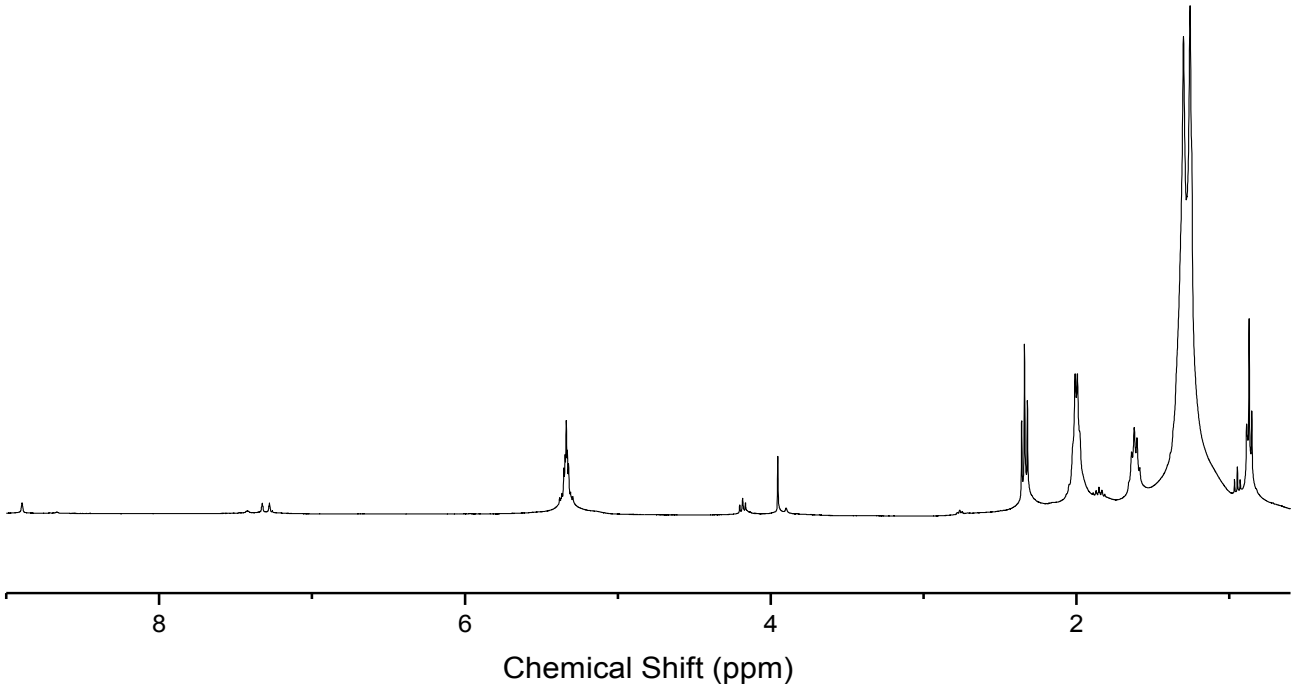

Figure 46. OA + $BMImBF_4$ ^{1}H-NMR Spectrum

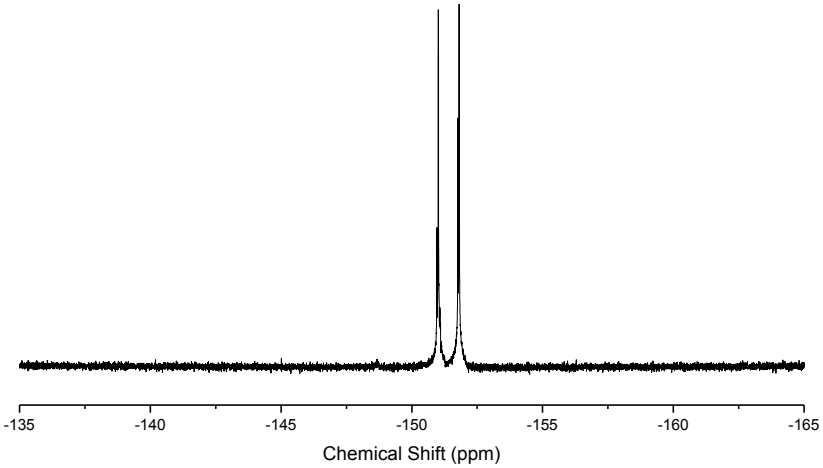

Figure 47. OA + $BMImBF_4$ ^{19}F-NMR Spectrum

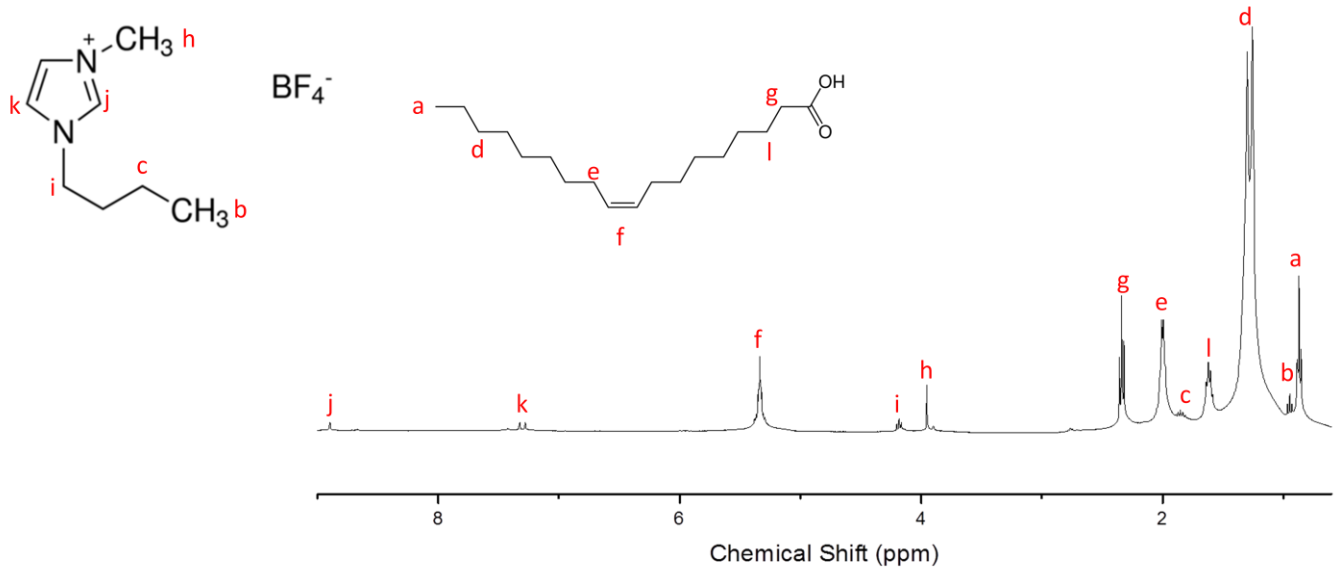

Figure 48. OA + $BMImBF_4$ ^{19}F-NMR Spectrum

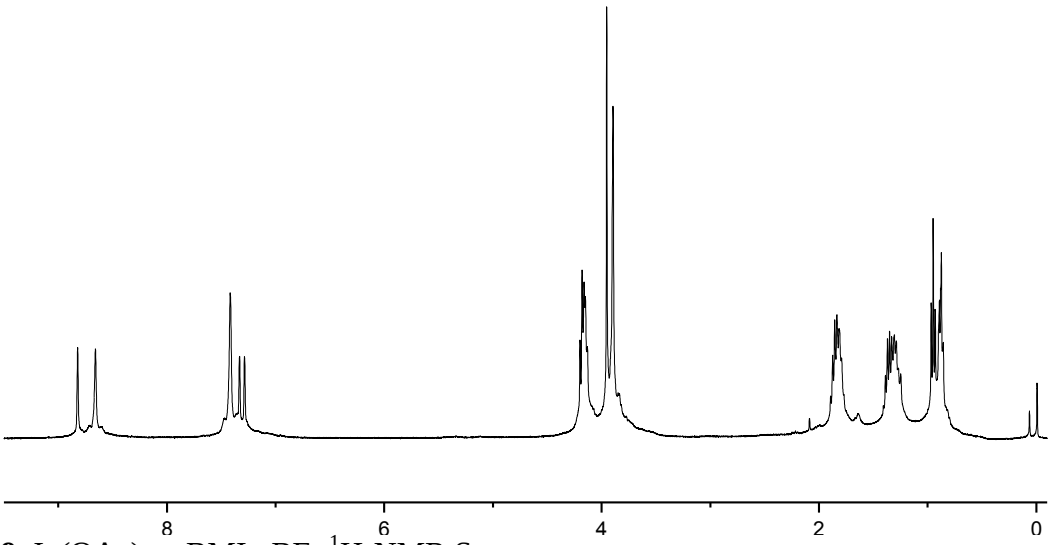

Figure 49. $In(OAc)_3$ + $BMImBF_4$ ^{1}H-NMR Spectrum

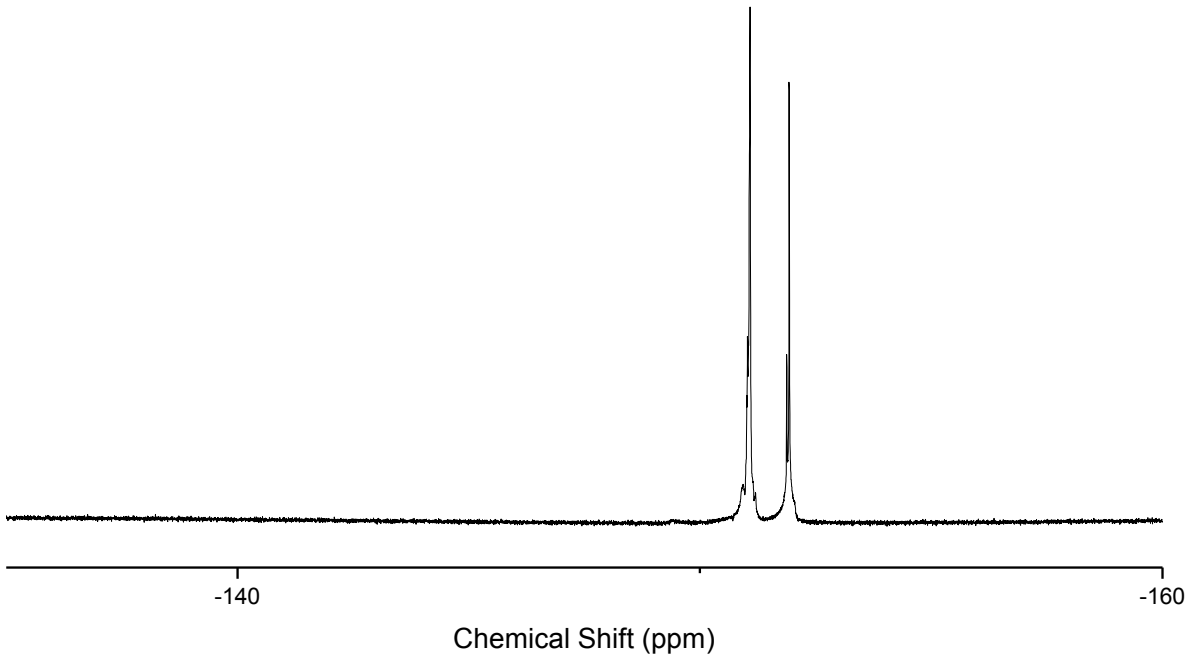

Figure 50. $In(OAc)_3$ + $BMImBF_4$ ^{19}F-NMR Spectrum

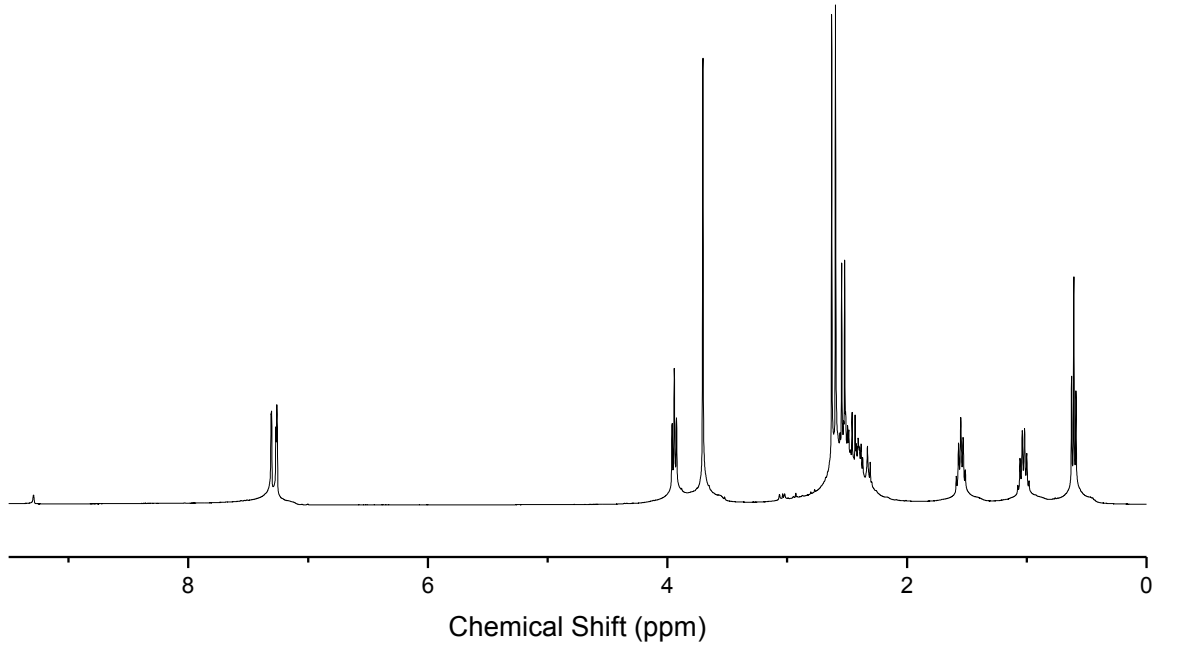

Figure 51. $P(NMe_2)_3$ + $BMImBF_4$ ^{1}H-NMR spectrum

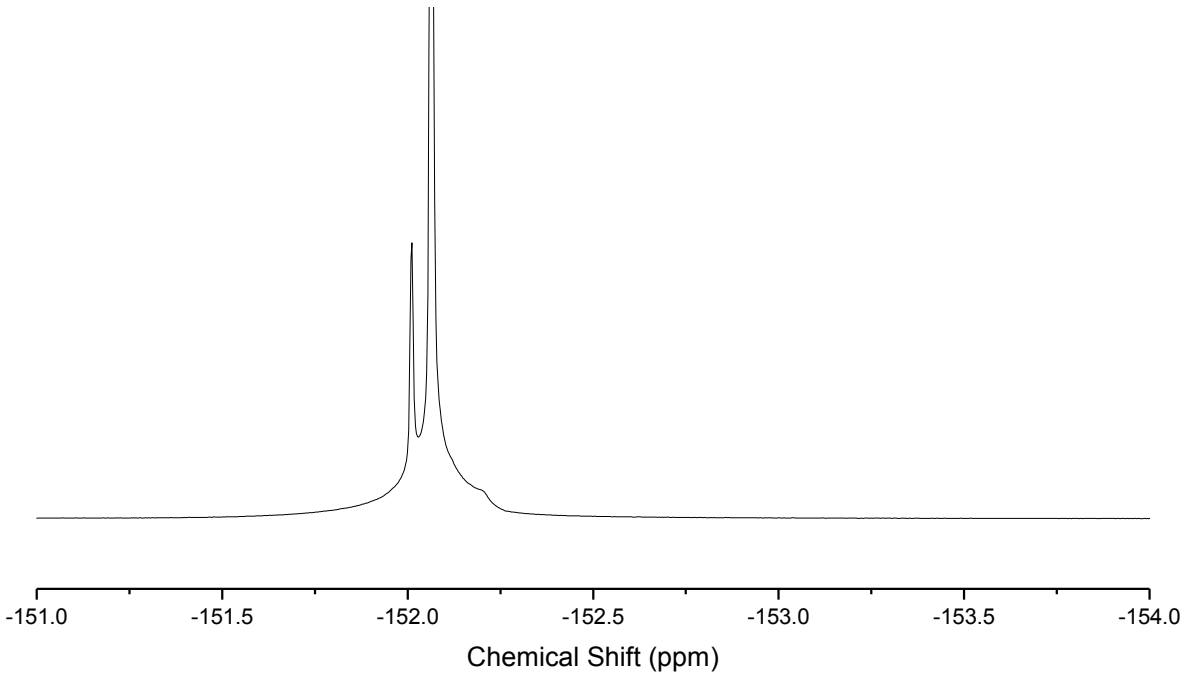

Figure 52. $P(NMe_2)_3$ + $BMImBF_4$ ^{19}F-NMR spectrum